[redacted]

Where are the « PeVatrons », the most extreme particle accelerators in our Galaxy ?

Gwenael Giacinti

(APC Paris, CNRS)

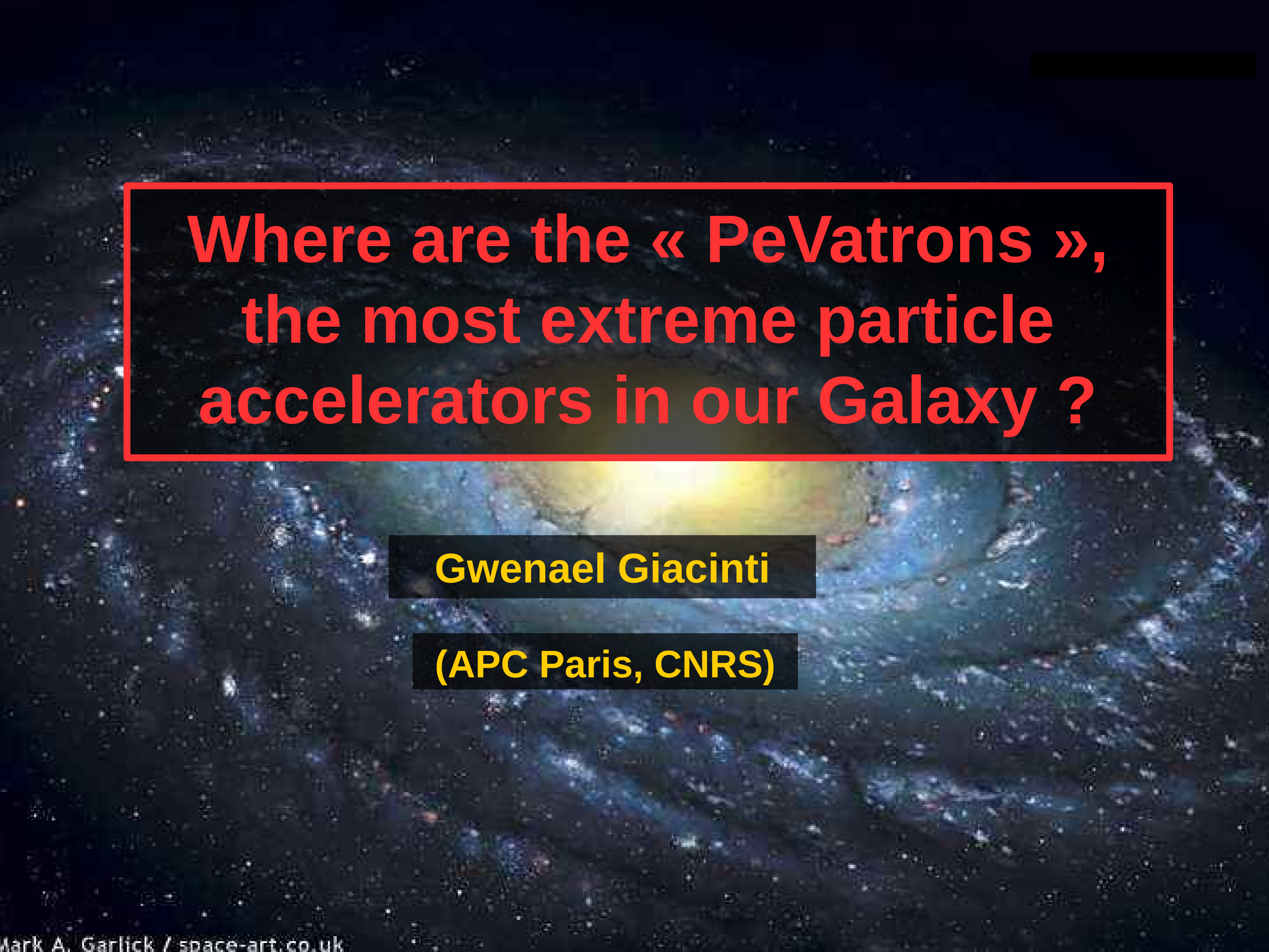

CR acceleration at supernova remnants

Diffusive Shock Acceleration

(Axford, Leer, & Skadron 1977, Krymsky 1977, Bell 1978, Blandford & Ostriker 1978)

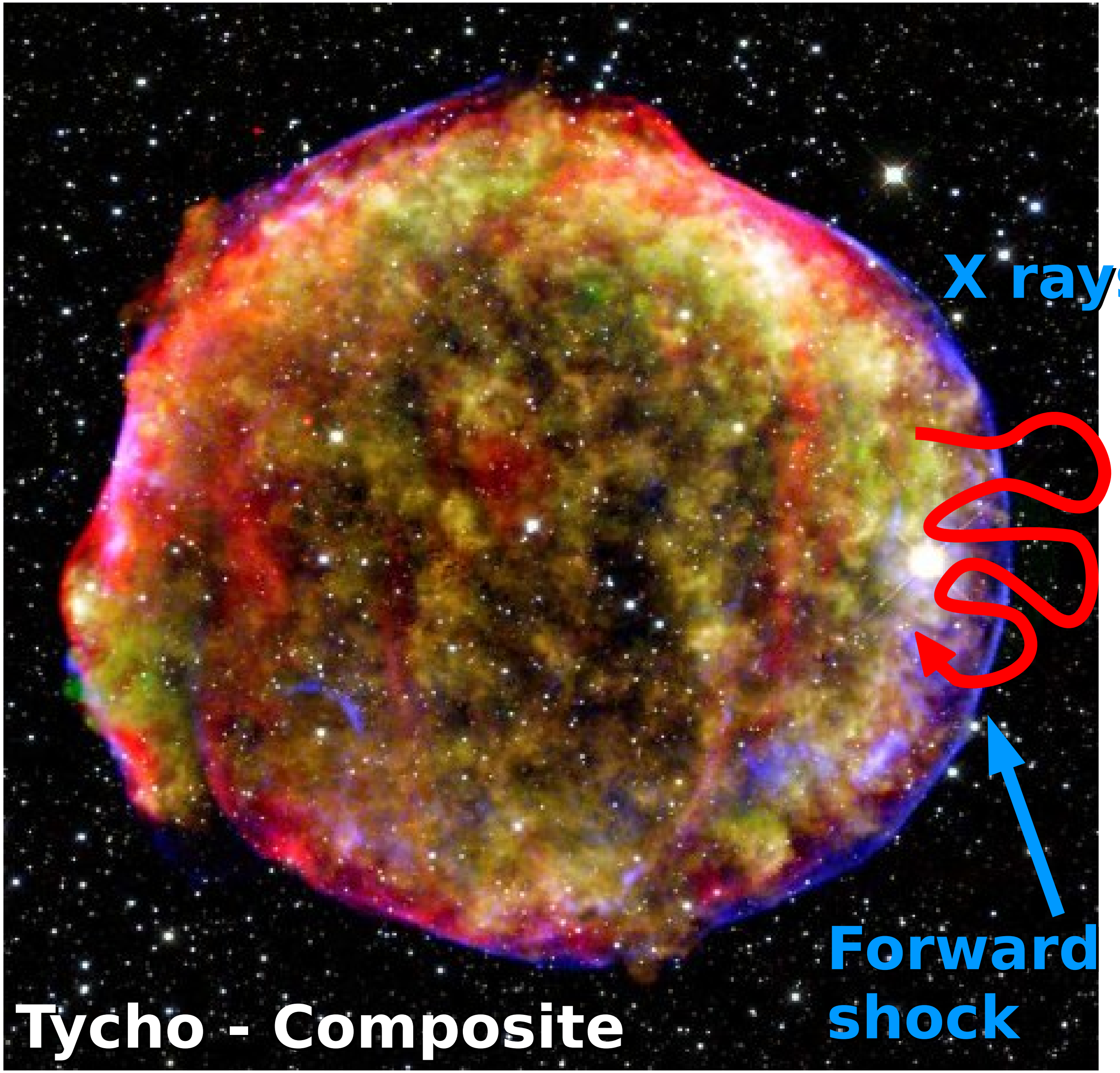

Diffusive shock acceleration: Plasma physics

Bell, Schure, Reville
& GG, MNRAS (2013) :

Hybrid simulations

=> **Standard SNRs do not reach beyond ~ 200 TeV**

=> Rare CC supernovae in dense winds could

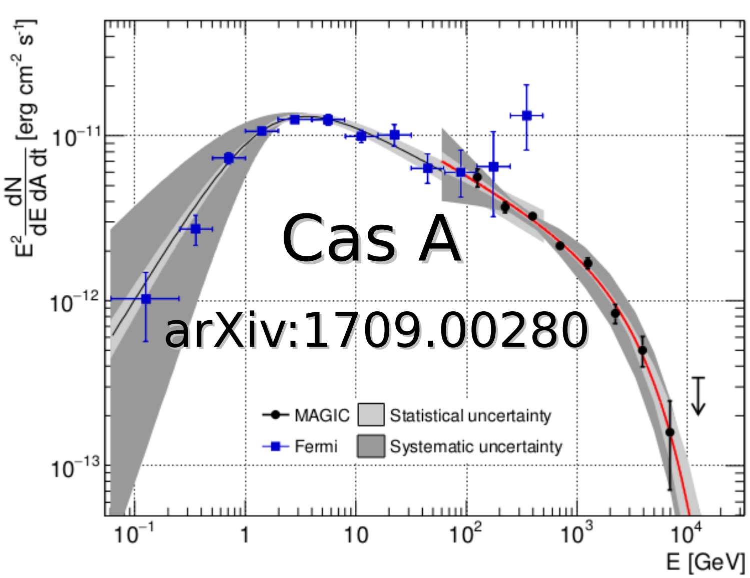

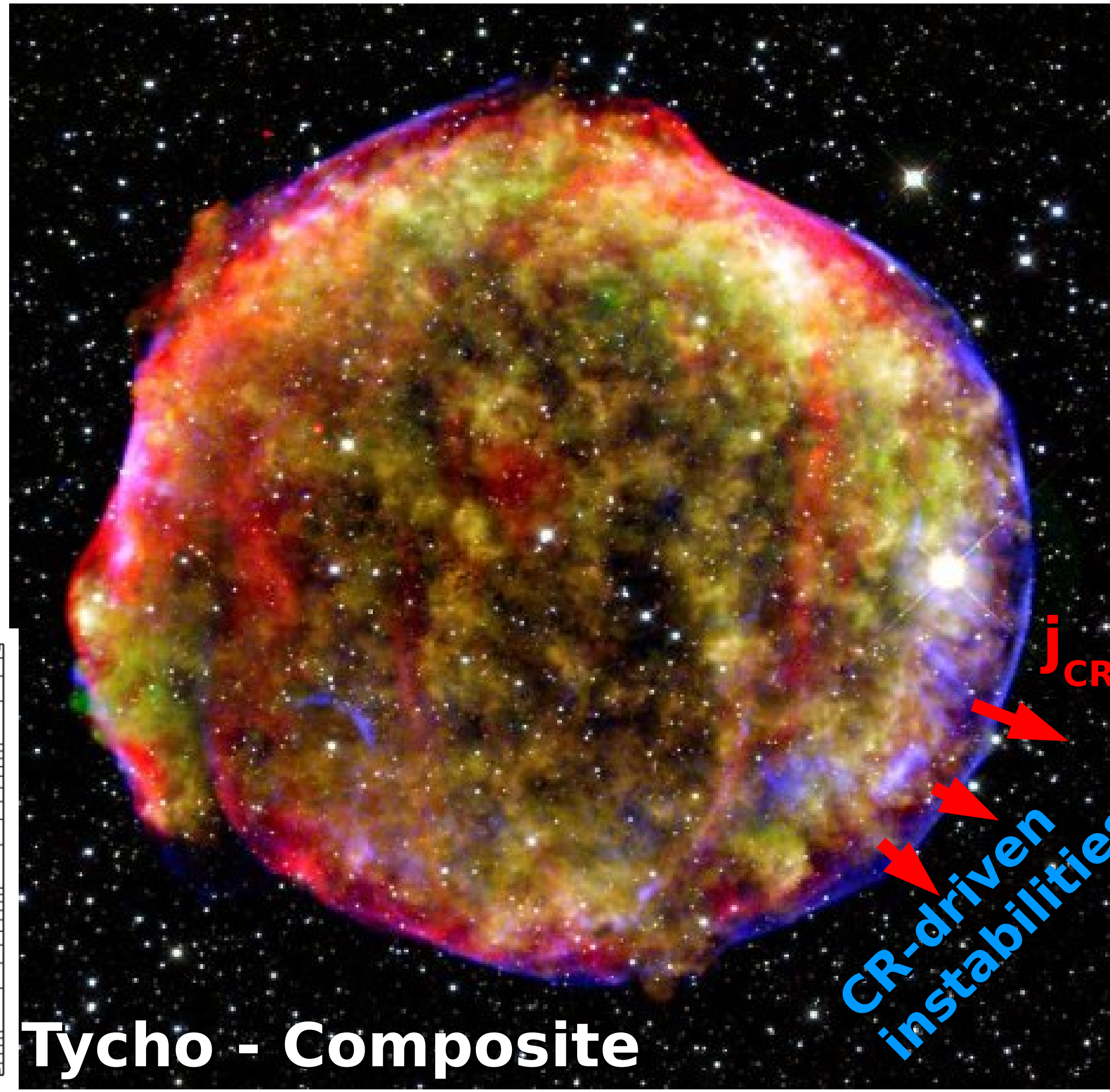

Sky at 25 TeV – 1 PeV with LHAASO

LHAASO Collaboration

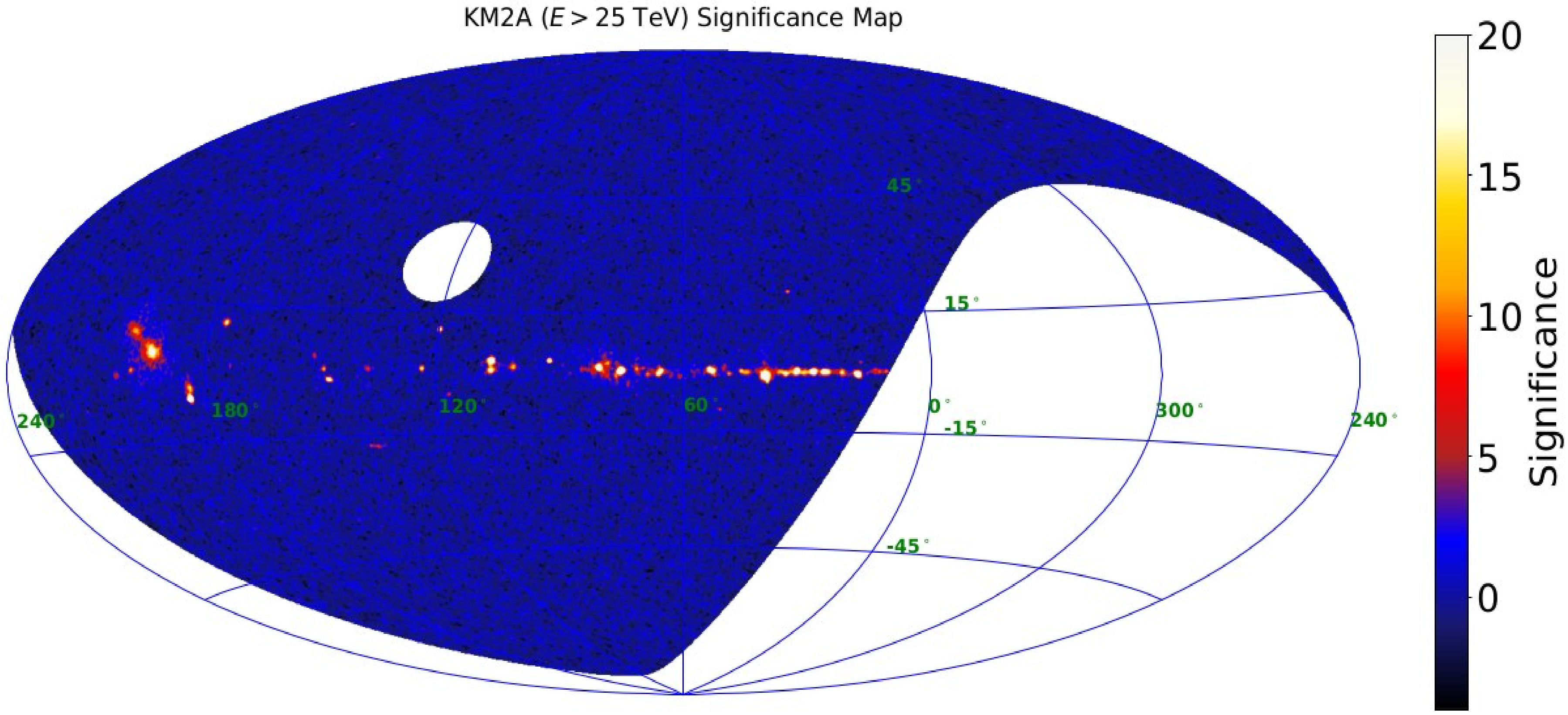

Dozens of PeVatrons

35 **PWNe and TeV halos** (leptonic) ; < ~ 7 **SNRs** (Hadronic) ? ;
dozens **unidentified** ; 6 **Microquasars** (Leptonic/Hadronic?)

Cas A not detected by LHAASO...

LHAASO Coll, Astrophys.J.Lett. 961 (2024) 2, L43

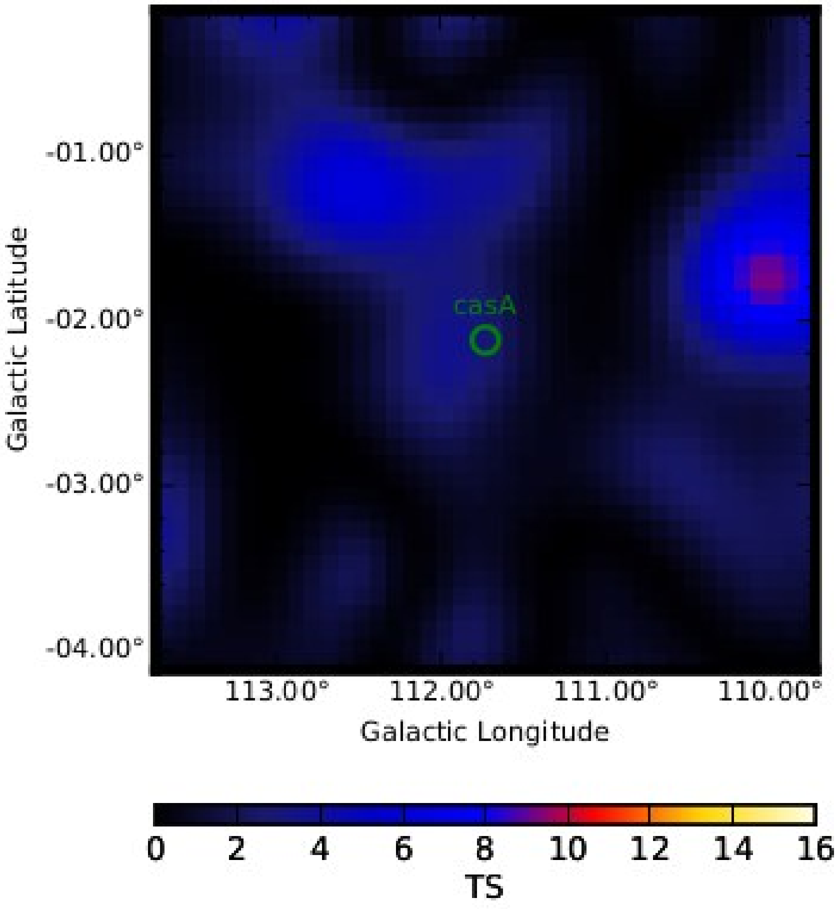

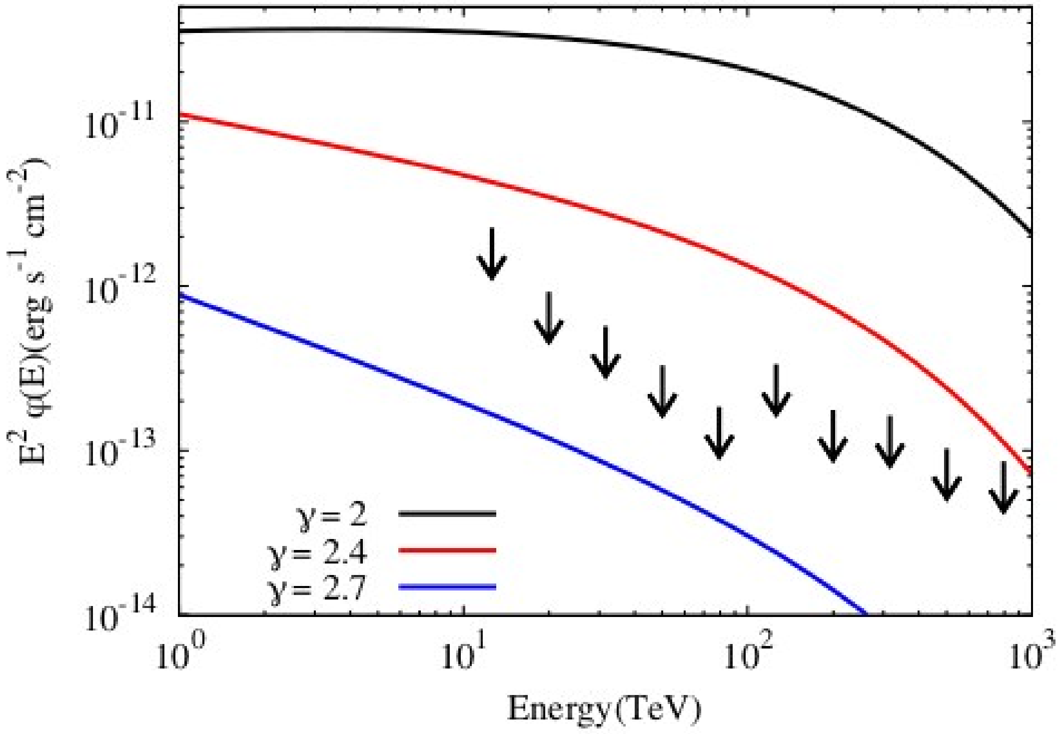

CRs cannot have traveled further than ~ 100 pc away

Radio SNe

THE ASTROPHYSICAL JOURNAL, 509:861–878, 1998 December 20

RADIO EMISSION AND PARTICLE ACCELERATION IN SN 1993J

CLAES FRANSSON[1] AND CLAES-INGVAR BJÖRNSSON[1]
Received 1998 April 27; accepted 1998 July 27

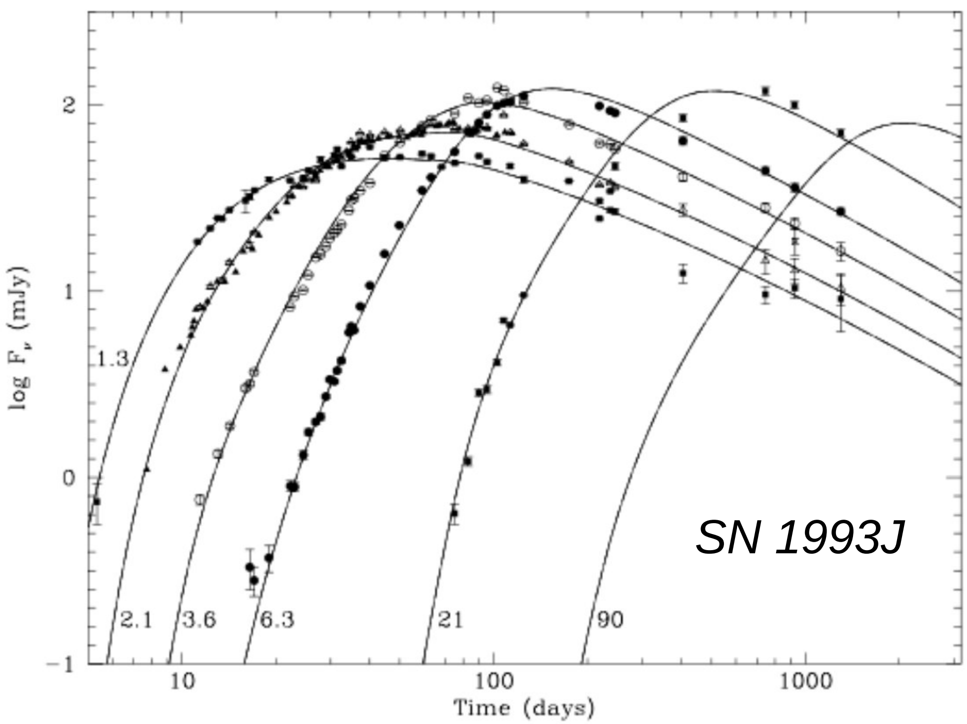

ABSTRACT

discussed. We find that a fit to the individual spectra by a
nal free-free absorption and synchrotron self-absorption, gives
ree-free absorption. A standard r^{-2} circumstellar medium is
om the flux and cutoff wavelength, the magnetic field in the
ock is determined to $B \approx 64(R_s/10^{15}\ \mathrm{cm})^{-1}$ G. The strength of
plification behind the shock. The ratio of the magnetic and
~ 0.14. Synchrotron losses dominate the cooling of the elec-
to photospheric photons are less important. For most of the
ectrum. A model where a constant fraction of the shocked,
ated, and subsequently lose their energy due to synchrotron
of the flux and number of relativistic electrons well. The
$^{2.1}$, consistent with diffusive shock acceleration. The injected
les with the thermal electron energy density, ρV^2, rather than
strongly connected to the deceleration of the shock wave. The
trons, if extrapolated to $\gamma \sim 1$, is $\sim 5 \times 10^{-4}$ of the thermal
quired is consistent with previous calculations of the circum-

Radio SNe

Astronomy & Astrophysics manuscript no. sn1993j
February 18, 2013

Radio emission and nonlinear diffusive shock acceleration of cosmic rays in the supernova SN 1993J

V. Tatischeff

Centre de Spectrométrie Nucléaire et de Spectrométrie de Masse, CNRS/IN2P3 and Univ Paris-Sud, F-91405 Orsay, France*
and Institut de Ciències de l'Espai (CSIC-IEEC), Campus UAB, Fac. Ciències, 08193 Bellaterra, Barcelona, Spain

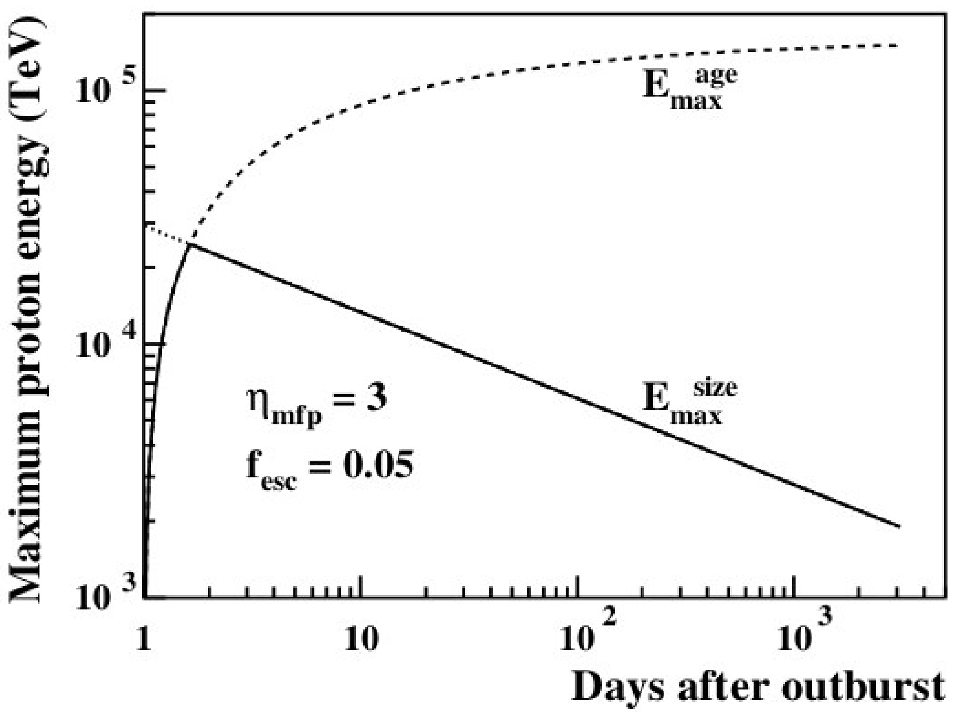

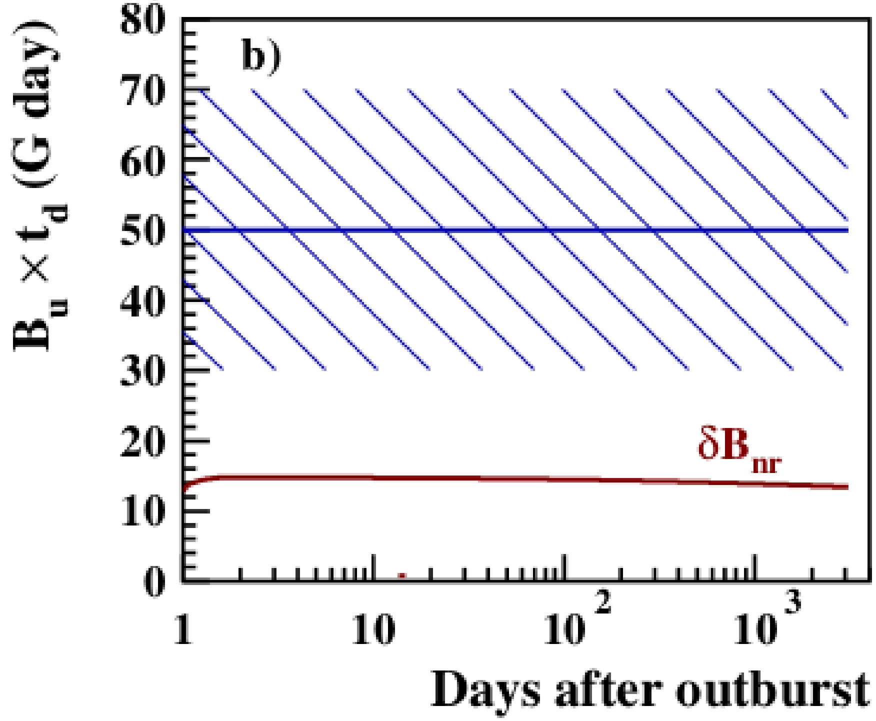

Young Massive Stellar Clusters ? (Superbubbles)

R136 (credit: NASA)

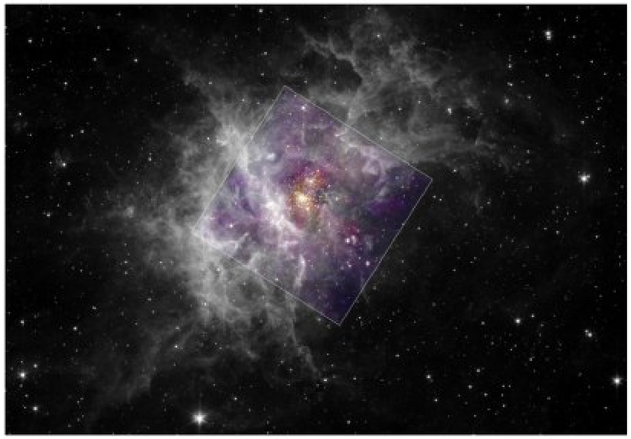

Westerlund 2 (credit NASA)

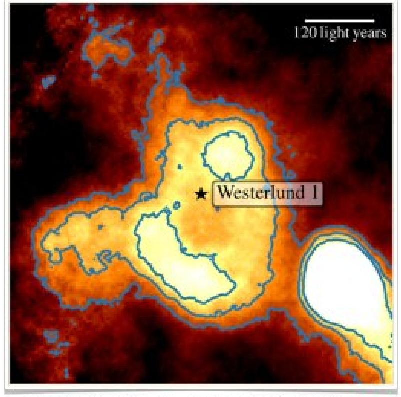

Westerlund 1 (credit HESS)

Weaver et al. (1977)

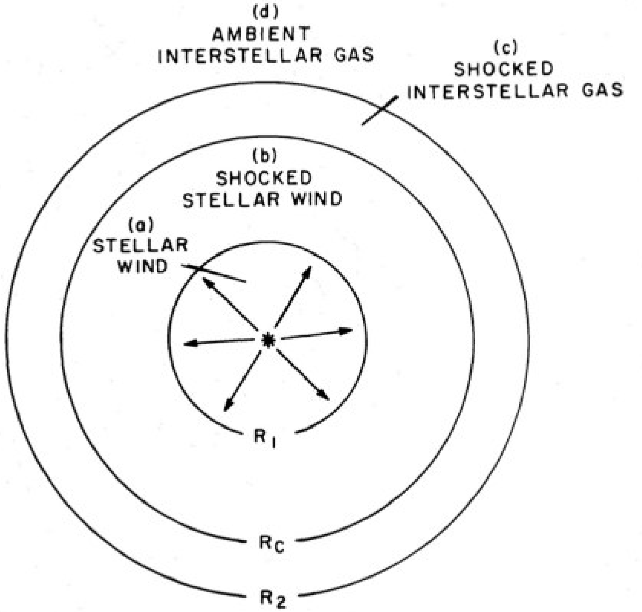

FIG. 1.—Schematic sketch indicating the regions and boundaries of the flow.

WR star winds : Similar energetic budget as SNe on Myr timescales.

Aharonian et al. (2019) + Several papers from Yang et al.

Young Massive Stellar Clusters ?

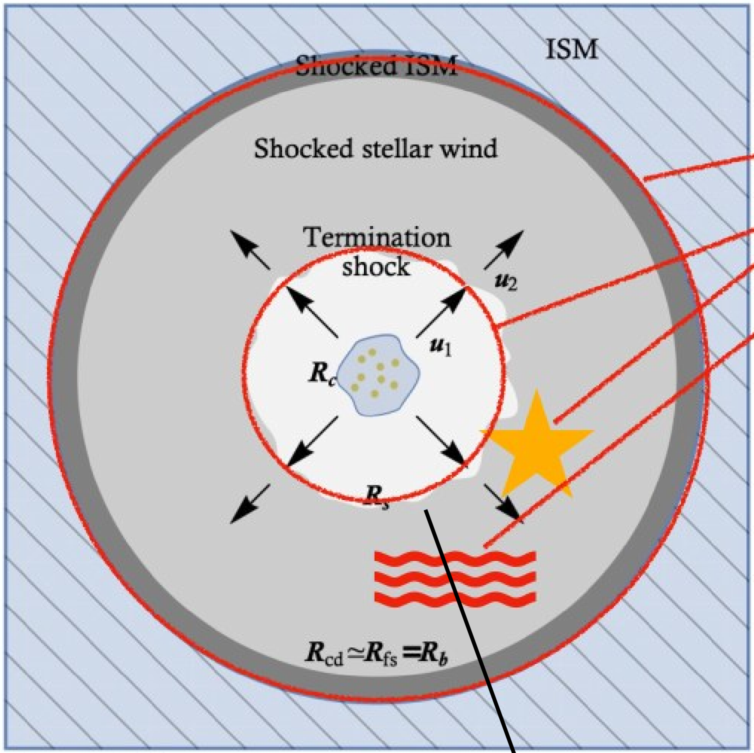

Morlino et al. 21

Acceleration mechanism	U [km/s]	B [μG]	R [pc]	E_{max}, canonical [PeV]	E_{max}, optimistic [PeV]
SB forward shock	30	1 – 10	50 – 100	0.01	0.1
SNR inside SB	3000	10 – 50	10 – 30	1	5
WTS around a compact cluster	2000	10 – 50	5 – 30	1	5
SNR embedded in a WTS	5000	10 – 50	5 – 30	5	10
HD turbulence	100	1 – 10	50 – 100	0.5	1
Collection of individual winds (loose cluster)	10 – 100	10 – 30	1 – 10	0.05	0.2

Table 1. Benchmark estimates of the maximum proton energy achievable via various acceleration mechanisms expected to take place inside superbubbles.

Vieu, Reville, Aharonian (2022)

Acceleration to > 10 PeV possible IF :

(1) Stellar winds turbulently amplify B fields in the cluster core to ~ 100 μG

(2) Massive stars produce long-lived supernova remnant shocks > 10,000 km/s

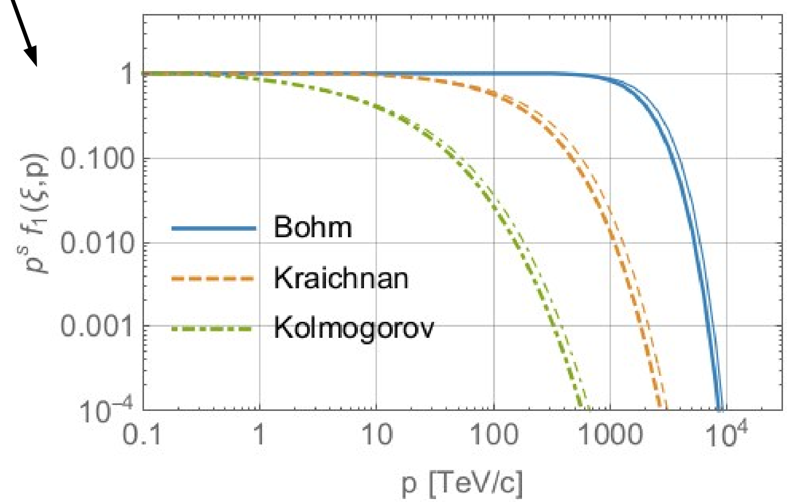

Morlino et al. (2021)

Cygnus OB2 (OB association) detected by LHAASO !

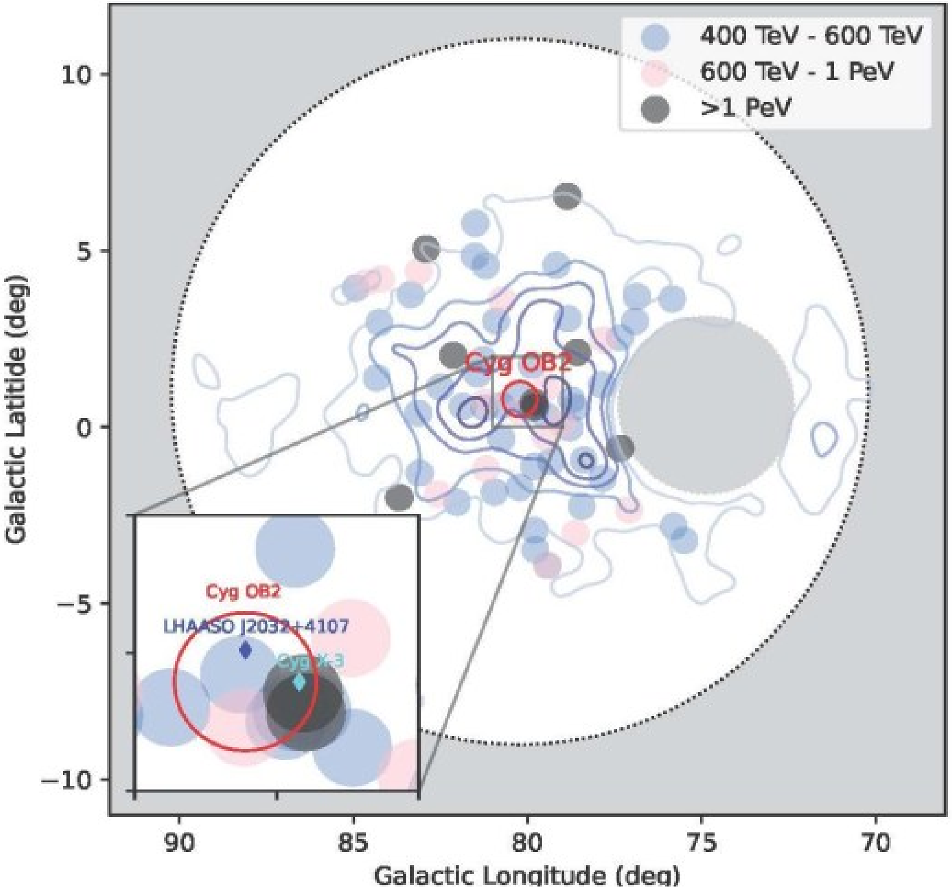

LHAASO Collaboration,
Science Bulletin (2024)

→ 8 gamma-rays above 1 PeV

→ Clear correlation with gas distribution

=> Hadronic origin

=> Protons with > 10 PeV energies !!!

=> SUPER-PEVATRON

… But how many YMSCs can accelerate to such extreme energies ?

Microquasars

Cygnus X1:

M_BH = $21M_o$

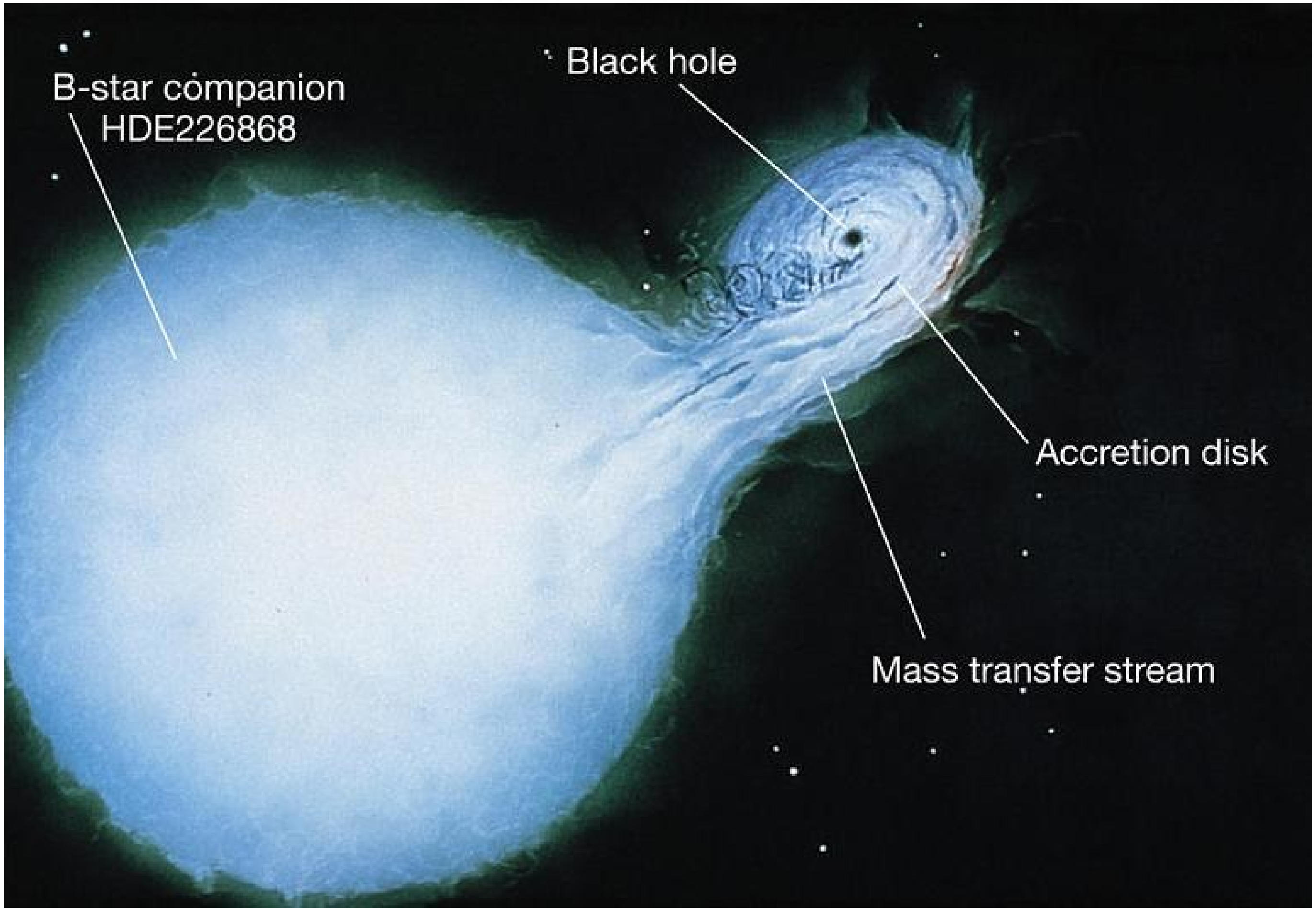

LHAASO's PeVatron microquasars

LHAASO Collaboration, National Science Review (2025)

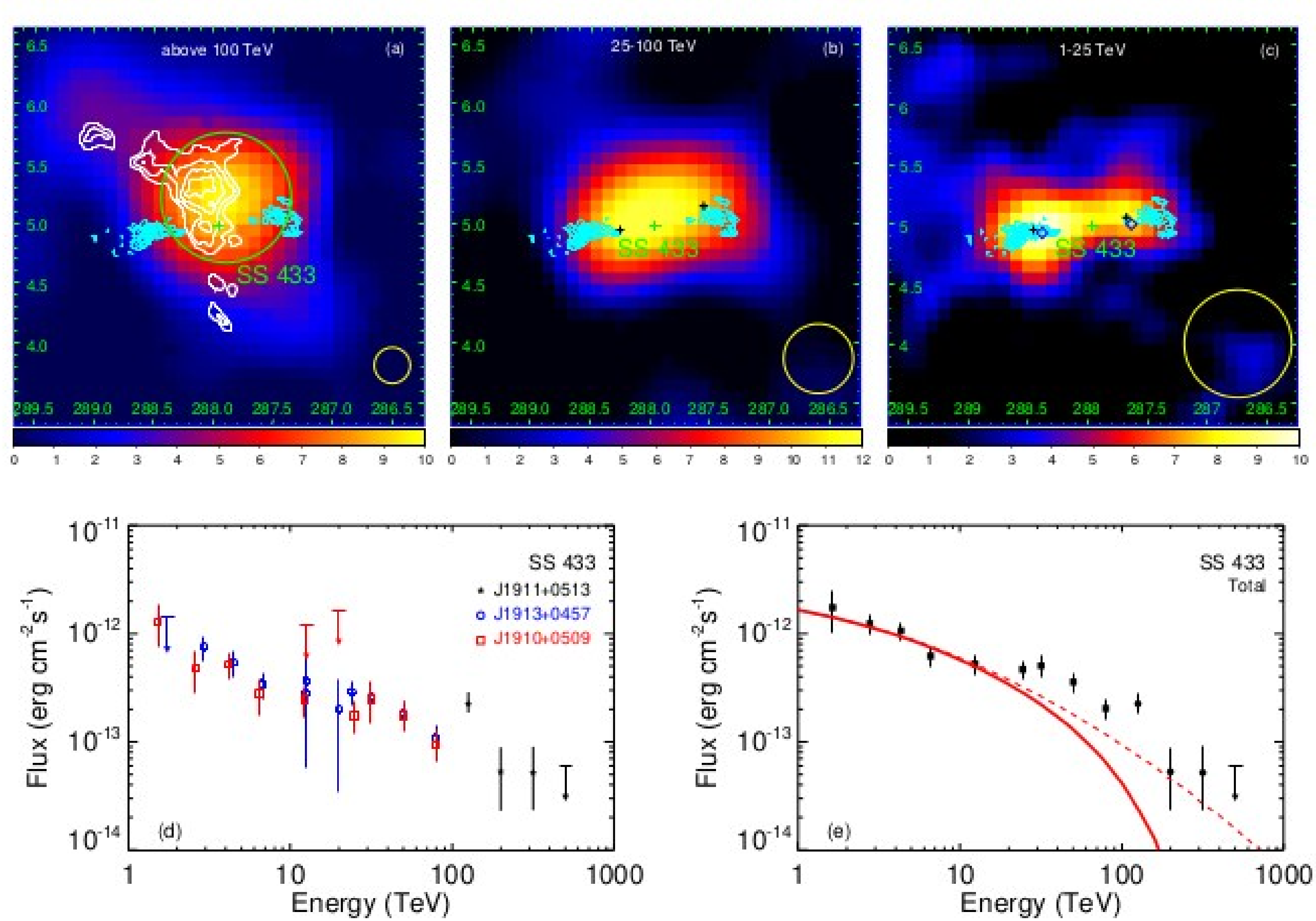

LHAASO's PeVatron microquasars

LHAASO Collaboration, National Science Review (2025)

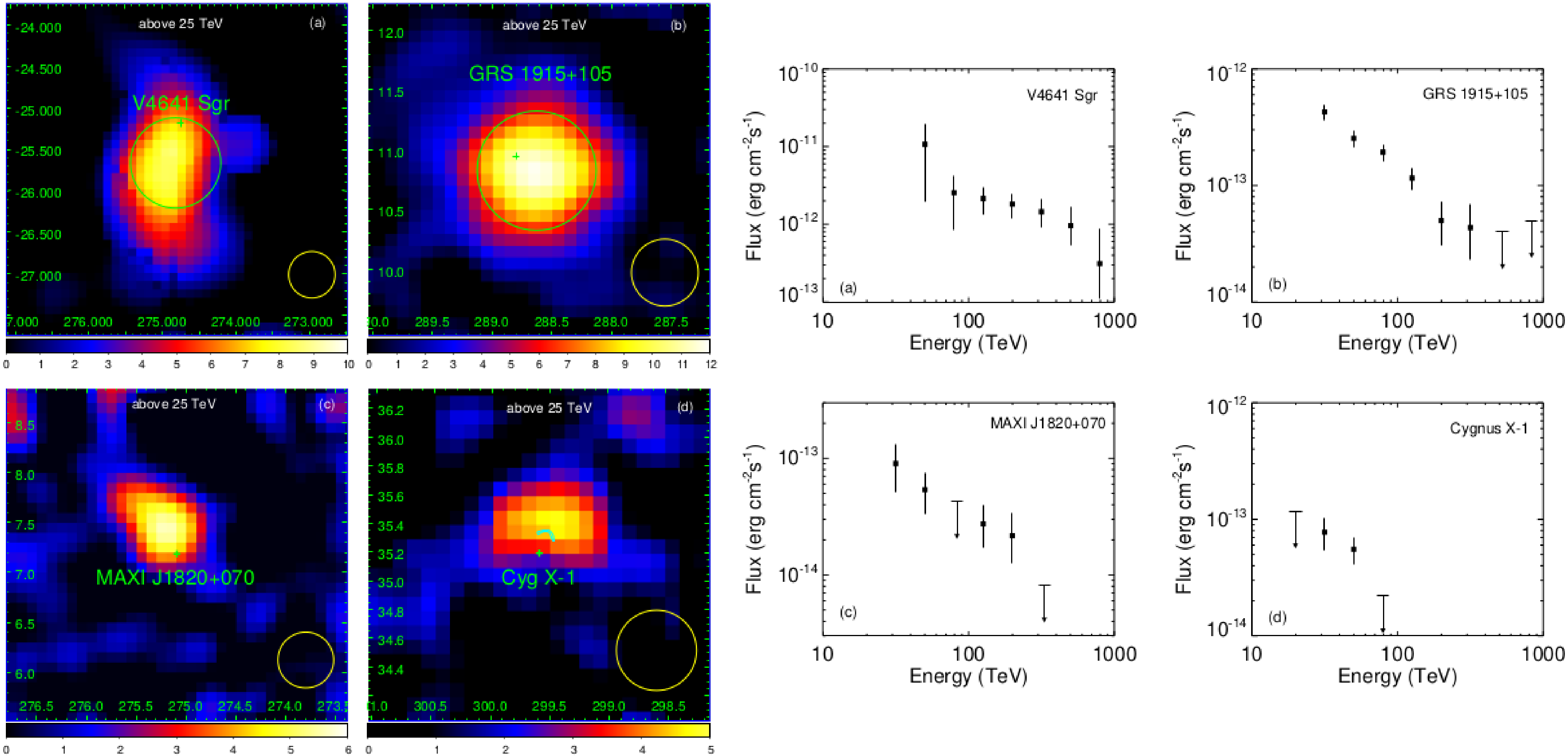

Cyg X3 P=4.8 h, 3 sigma

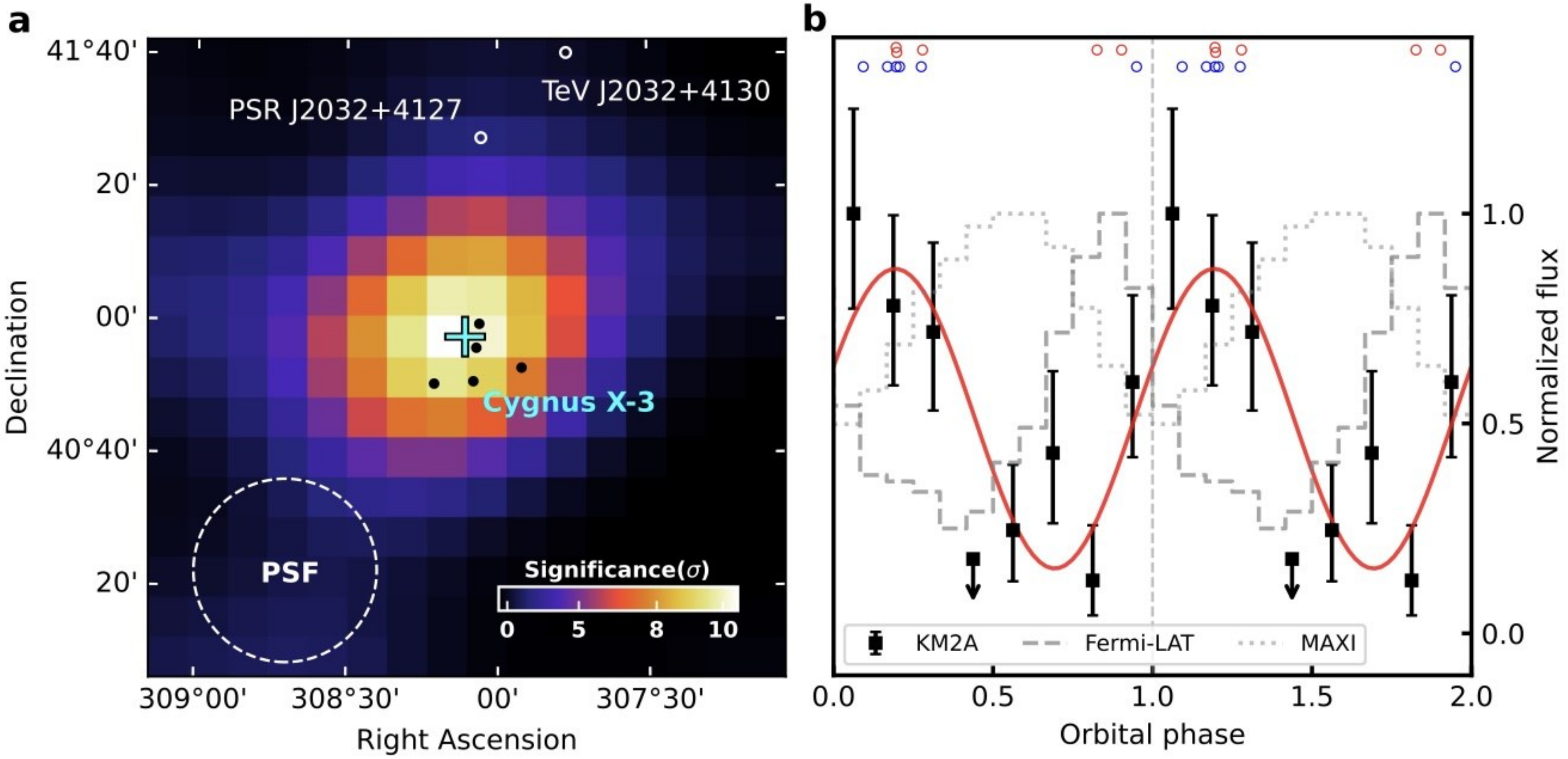

LHAASO collaboration, 2512.16638

Highest energy photon detected from any source in the sky E = 3.7 PeV

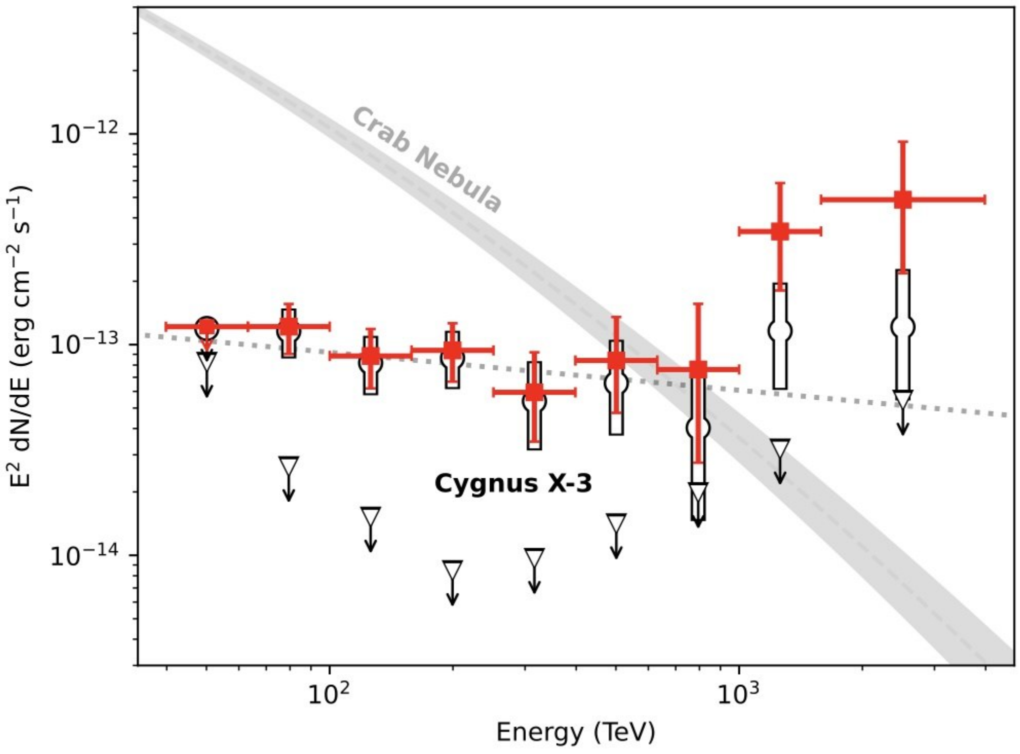

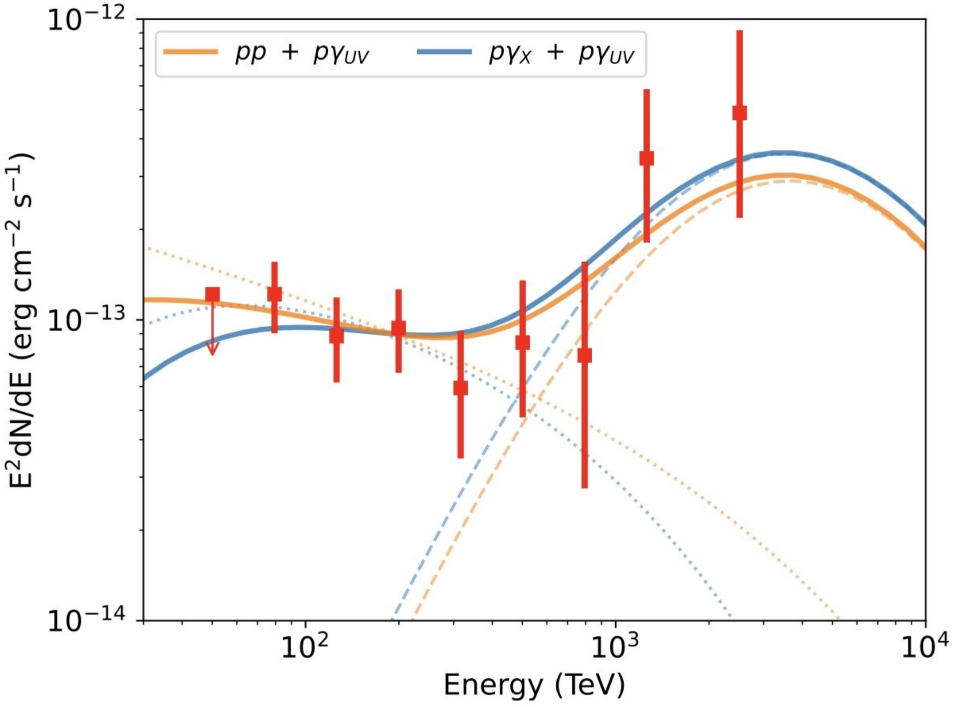

LHAASO collaboration, 2512.16638

Acceleration mechanism?

RESEARCH

GAMMA-RAY ASTRONOMY

Acceleration and transport of relativistic electrons in the jets of the microquasar SS 433

H.E.S.S. Collaboration*†

H.E.S.S. Collaboration,
Science **383**, 402–406 (2024)

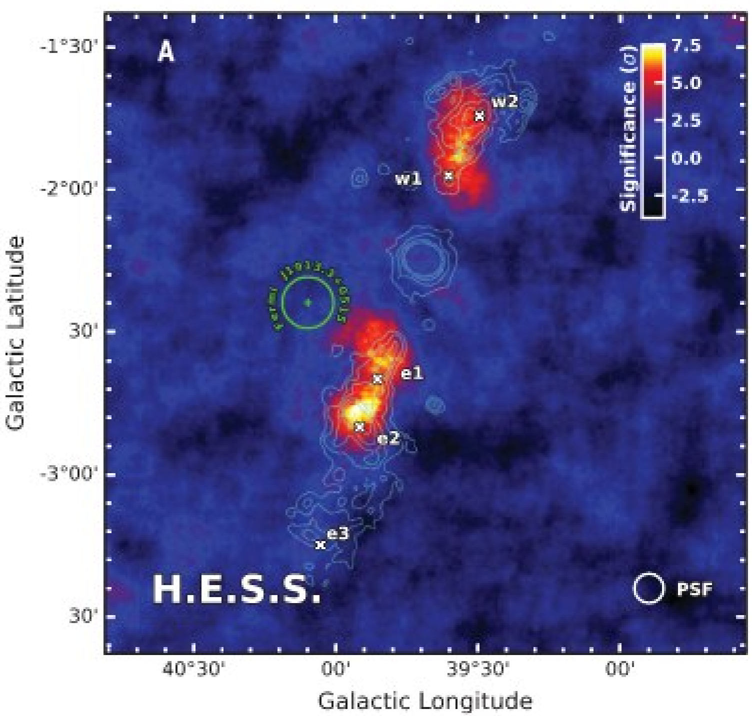

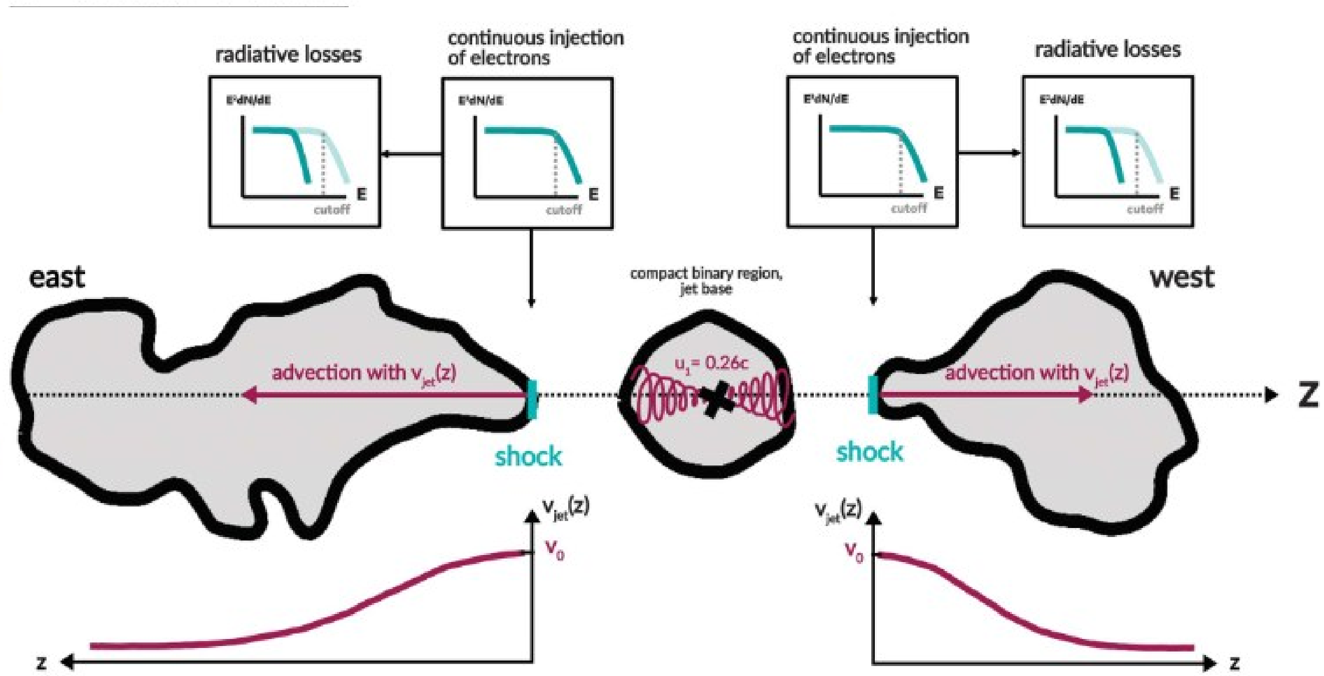

In-situ particle acceleration, to > 100 TeV.

Safi-Harb et al. (2022)

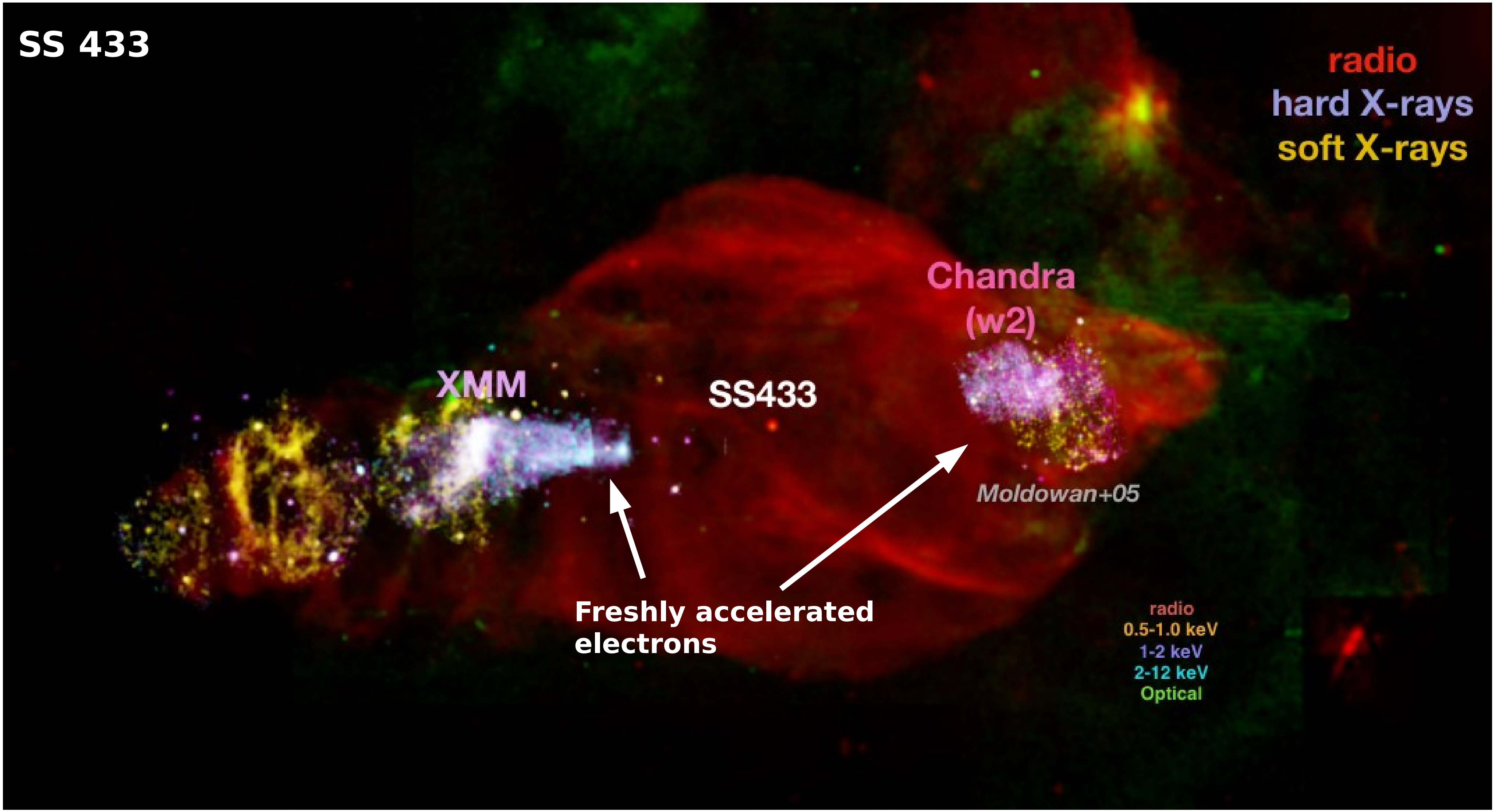

Active galaxies & their jets – FR II

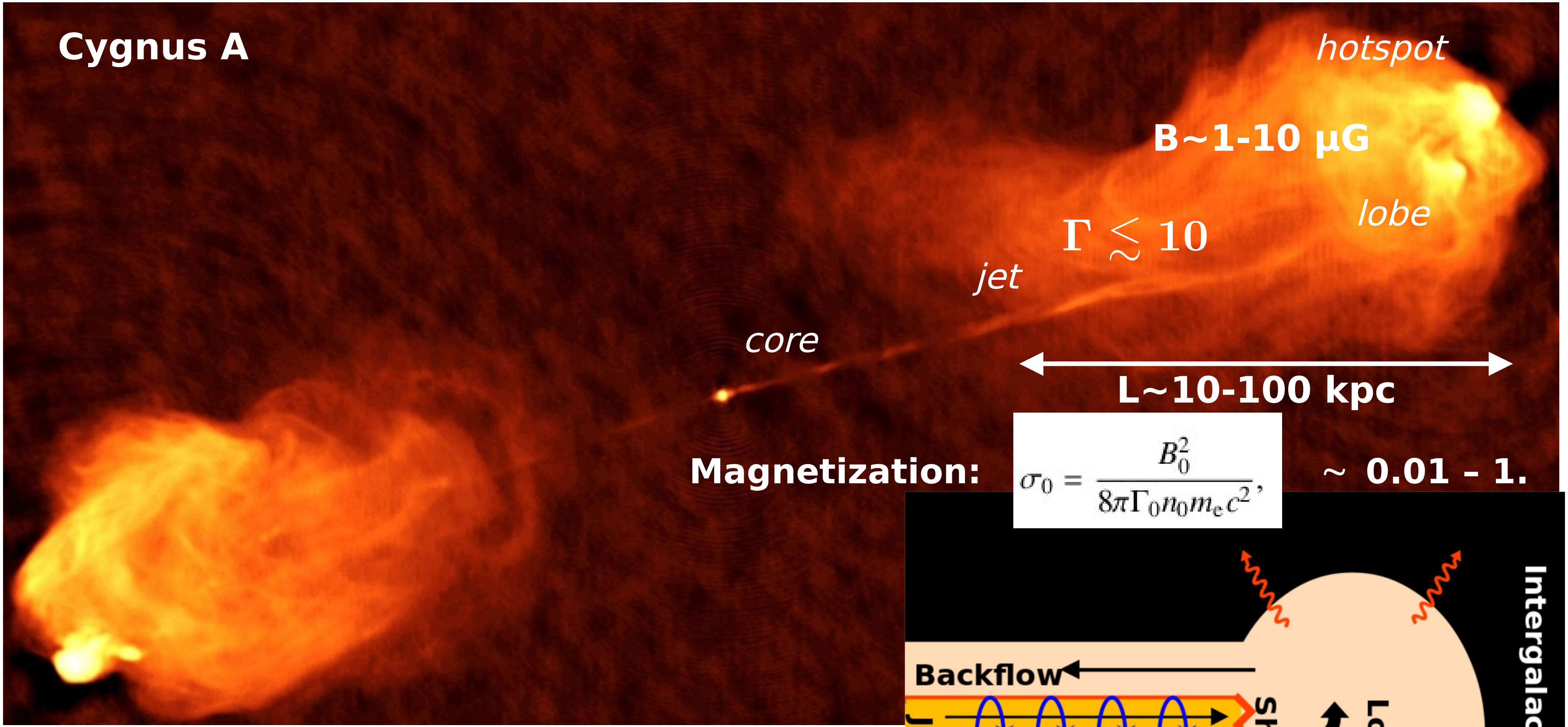

Magnetization: $\sigma_0 = \frac{B_0^2}{8\pi\Gamma_0 n_0 m_e c^2}$, ~ 0.01 – 1.

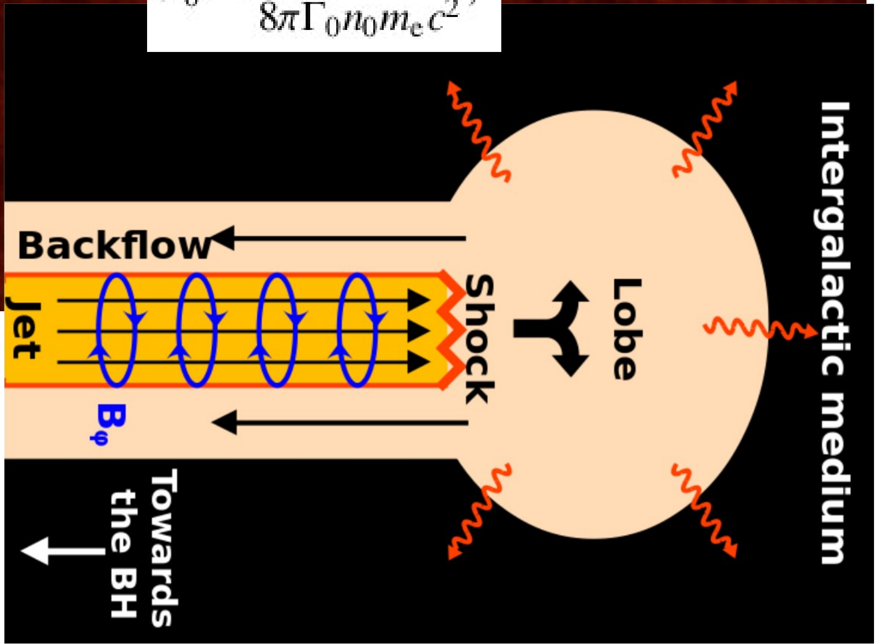

Relativistic shocks: Bednarz & Ostrowski (1998); Kirk et al. (2000); Achterberg et al. (2001)

Particle-In-Cell (PIC) simulations

→ <u>**Unmagnetized case**</u> **(σ=0):**

Spitkovsky (2008), Sironi + (2013), Plotnikov+ (2018), Lemoine+ (2019)

Relativistic unmagnetized shocks
Good but slow accelerators.

Maximum energy grows as $t^{1/2}$
(Reville & Kirk 2010, Plotnikov et al. 2013)

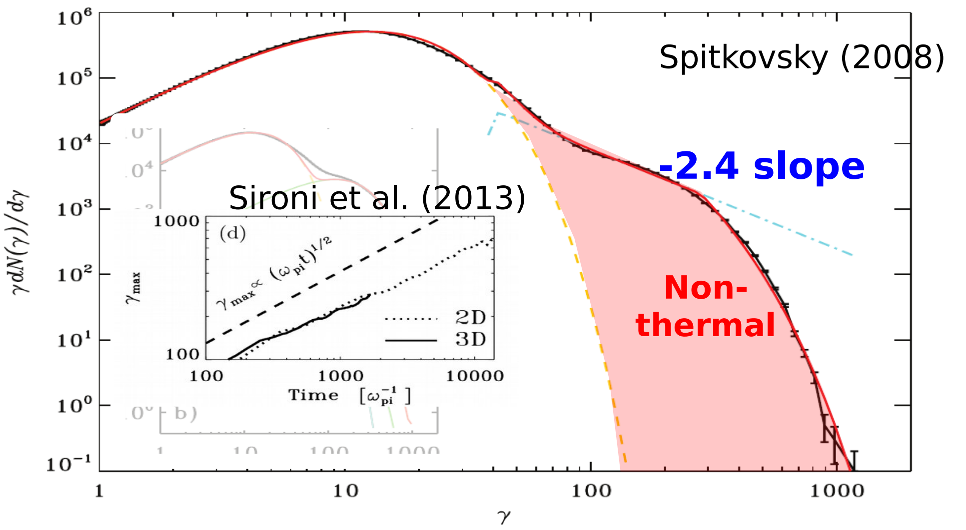

→ <u>**Magnetized case**</u> **(σ>10^{-3}):**

Even weak magnetization levels stop particle acceleration.

E_{max} quickly saturates.

Cannot accelerate to VHE!

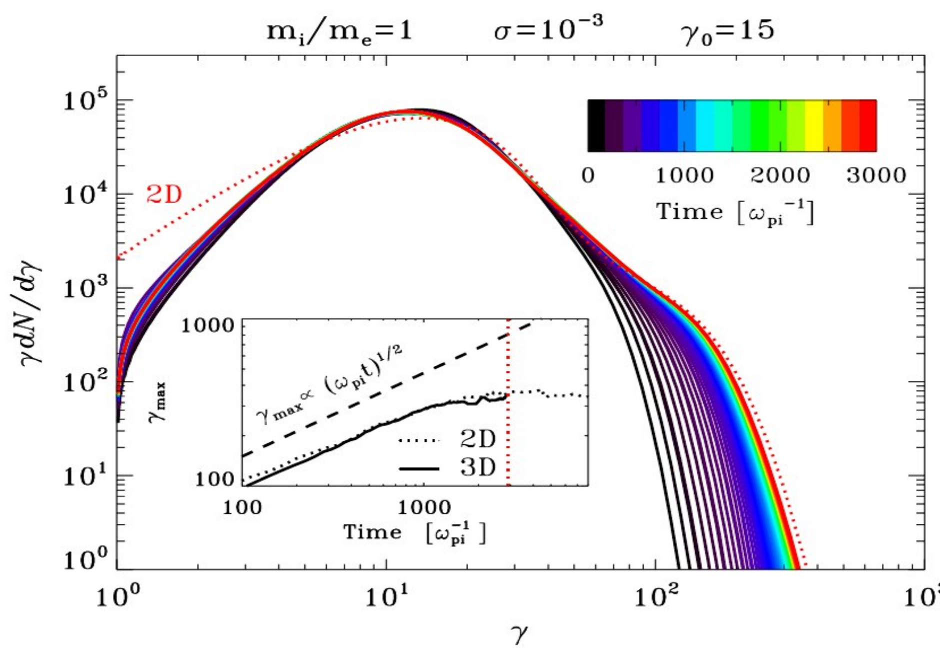

Sironi et al. (2013)

Solution: Global B field geometry

LARGE-SCALE GEOMETRY OF THE B FIELD MAY SOLVE THE PROBLEM!

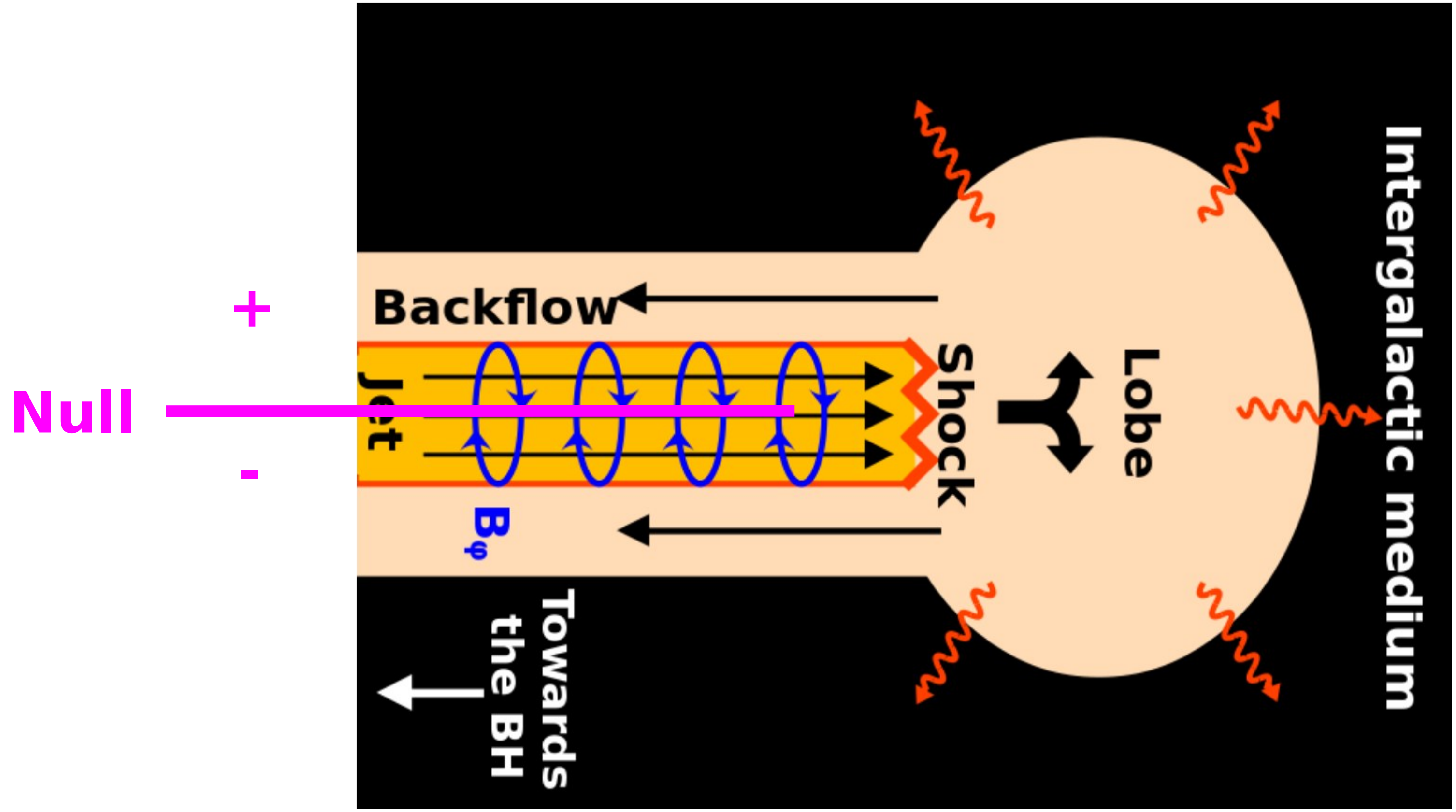

Cerutti & Giacinti, A&A (2023)

Particle-In-Cell (PIC) setup

2D Cartesian box (xz-plane), **262,144×16,384 cells, or 6554x410 d_i (ion skin depth)**

Electron-ion plasma with **m_i/m_e=25**

Magnetization : **σ=0.1, 1**

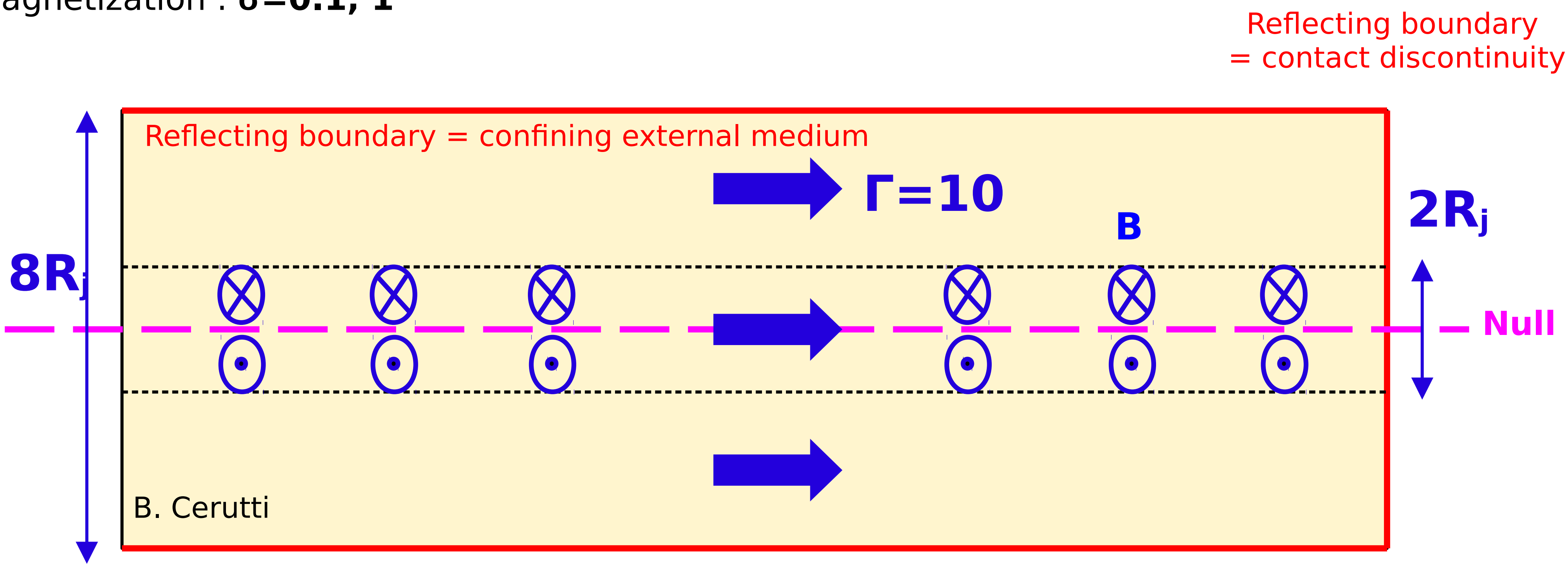

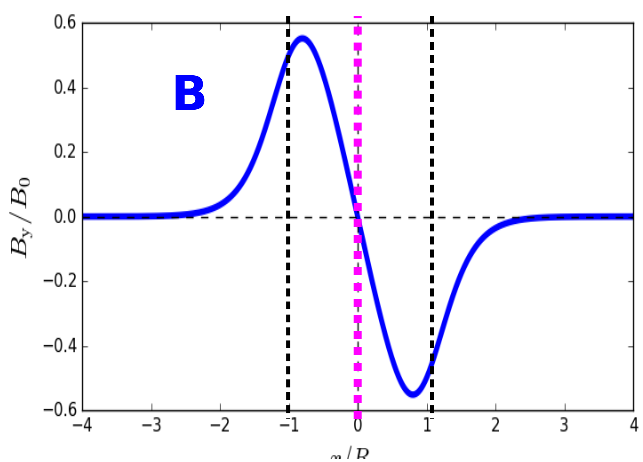

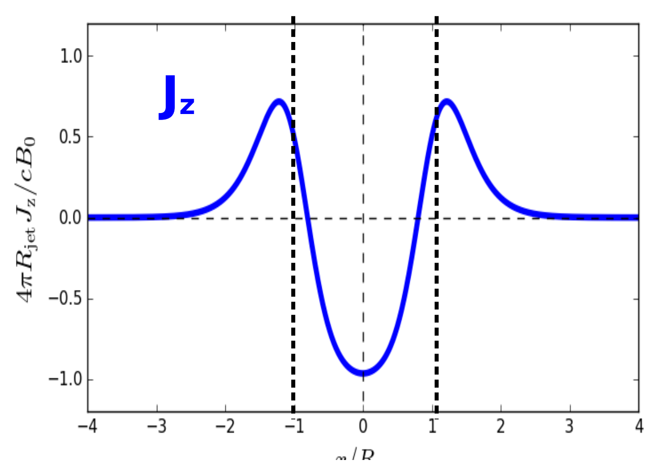

Results PIC : Density evolution

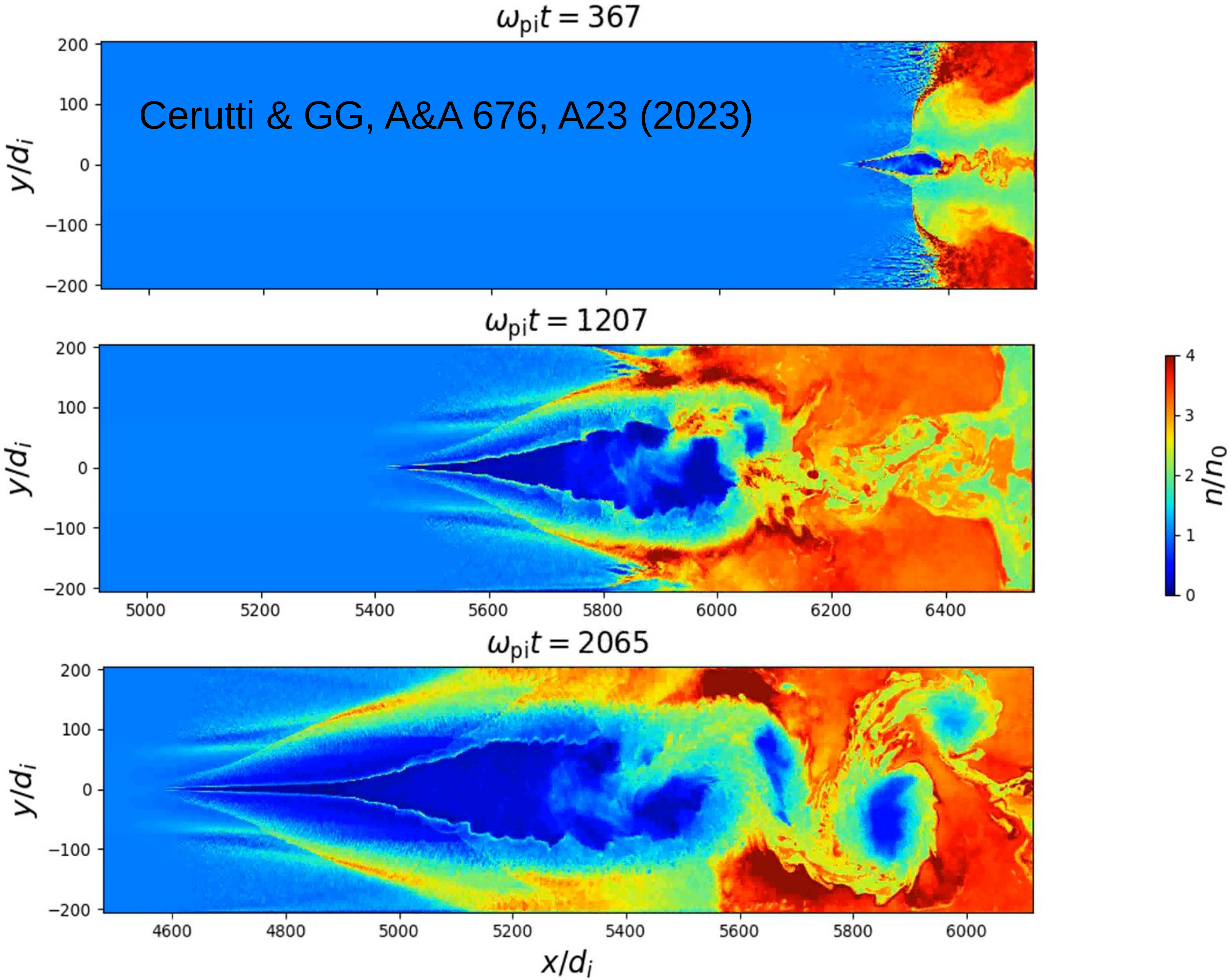

Results – PIC Simulations

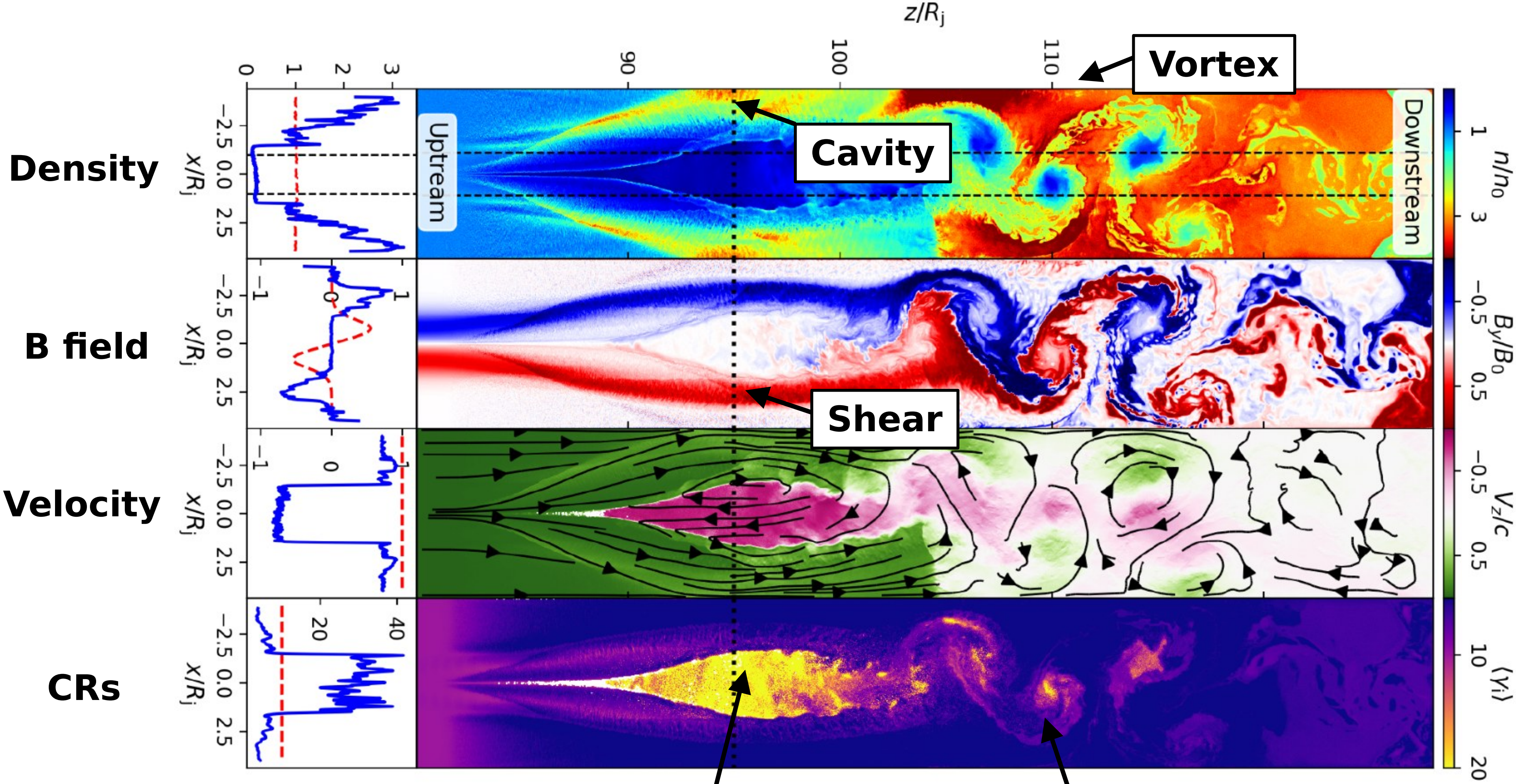

Cerutti & GG, A&A 676, A23 (2023)

HE particle <u>acceleration</u>

HE particle <u>escape</u>

→ Shear-flow acceleration at the edges of the cavity

Ion spectrum: Time Evolution & E_{max}

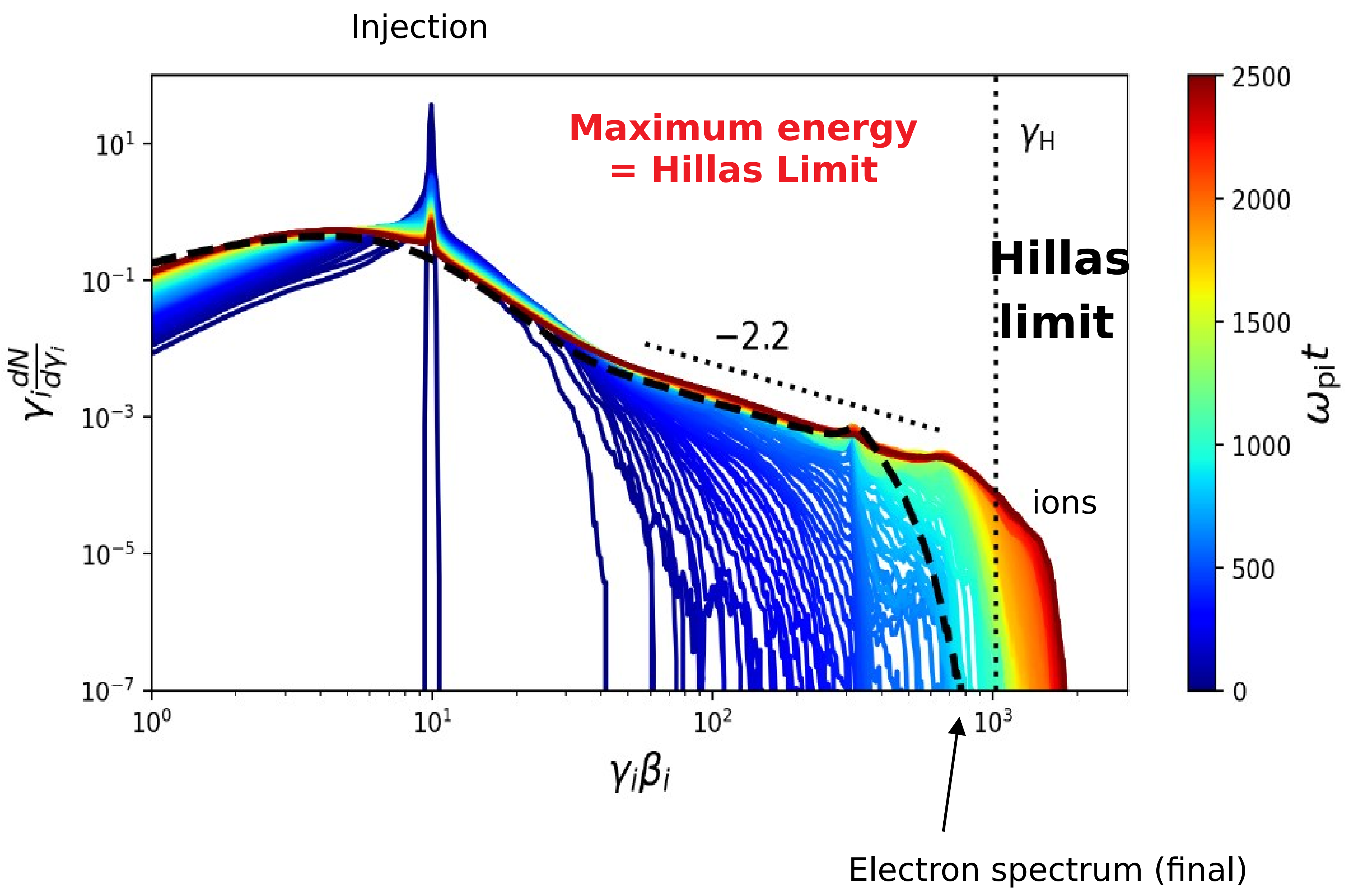

Constraints on hadronic emission from microquasars detected by LHAASO

Vecchiotti, Amato, GG, Morlino & Peron, A&A (2026)

→ Do 100TeV gamma-rays originate from hadronic interactions of accelerated CRs with the ambient/source medium ?

→ Contribution of these sources to the measured CR proton spectrum around the knee ?

→ CR propagation in the source vicinity diffusion-dominated, with a D=Dgal/100 close to the source. Gas : H_2 (Dame et al. 2001), and HI (HI4PI Collaboration et al. 2016)

→ Continuous injection over timescales of t age = 0.1 − 1 Myrs.

Results :

→ Hadronic interactions alone cannot fully account for the observed emission for any of the LHAASO sources. For GRS 1915+105 and MAXI J1820+070, the hadronic scenario can work with acceleration efficiency > 10%.

→ Detected sources contribute < 4% of the CR flux at 1 PeV for an injection timescale of 0.1 Myr and a CR acceleration efficiency of 10%.

→ For maximum acceleration efficiency allowed by gamma-ray observations, contribution of these microquasars to the CR flux at PeV: 37%.

→ ~ 1 Myr injection timescales : Contributions exceed the observational constraints.

→ Sources not detected at UHE, maximum contribution of ~ 17%.

Constraints on hadronic emission from microquasars detected by LHAASO

Vecchiotti et al., A&A (2026)

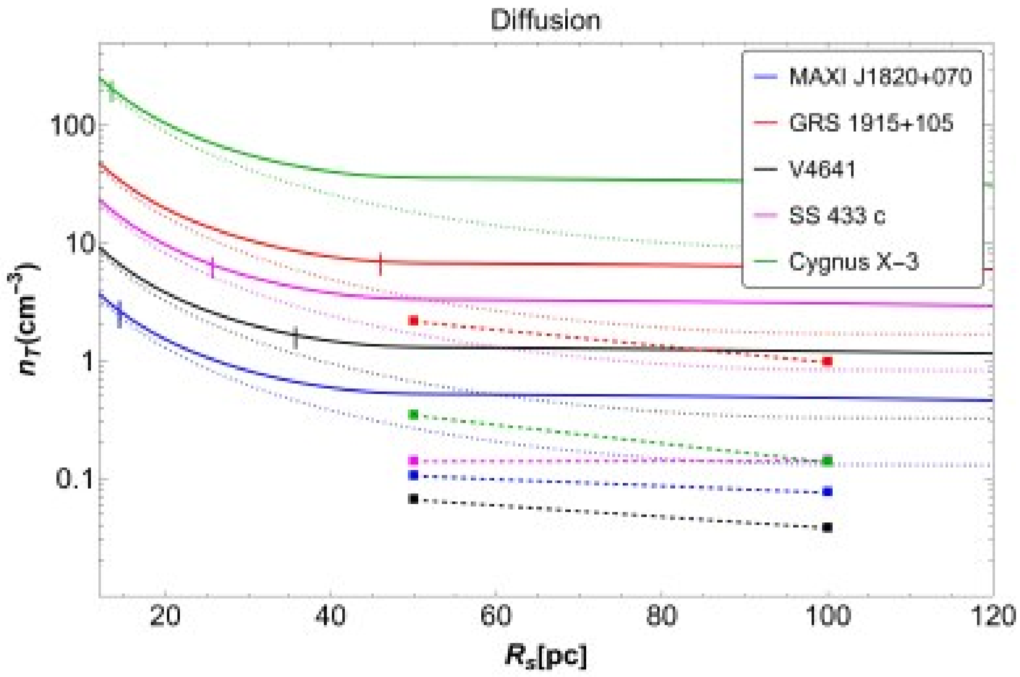

Fig. 2: Estimated target density required to reproduce the gamma-ray emission at 100 TeV as a function of R_s, the radius of the interaction region, for the microquasars detected by LHAASO. The estimates are shown as solid (dotted) lines for

Constraints on hadronic emission from microquasars detected by LHAASO

Vecchiotti et al., A&A (2026)

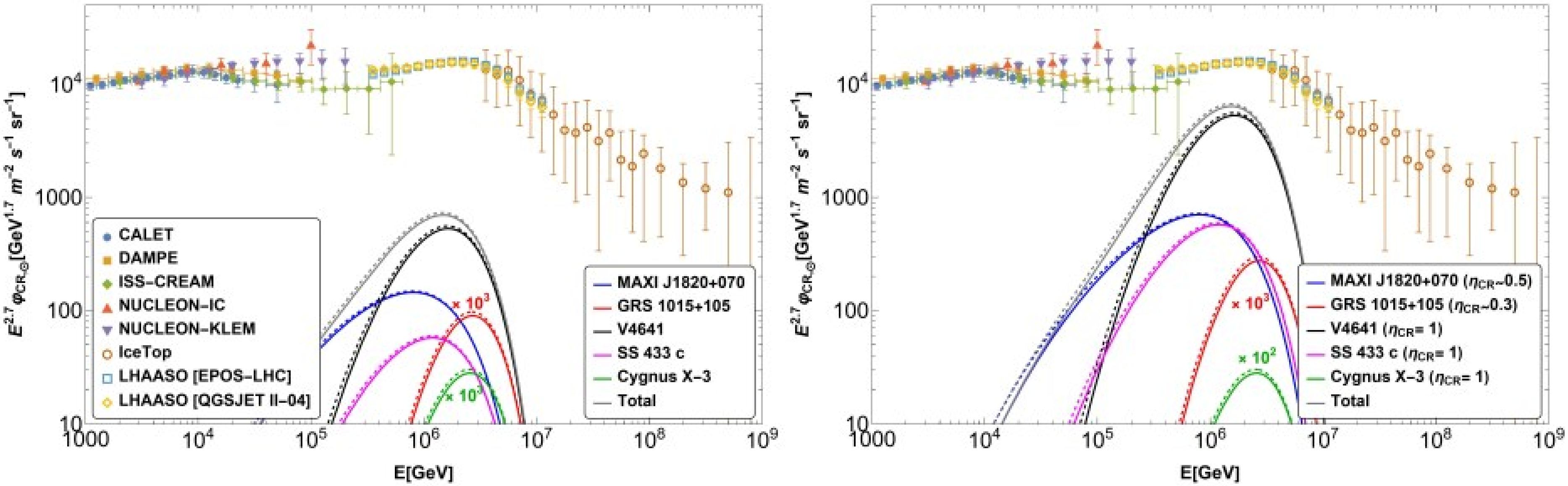

Fig. 3: Contribution to the CR proton spectrum for the microquasars detected by LHAASO in the diffusion-dominated two-zone model assuming continuous injection over 100 kyr (solid lines), compared with proton data from LHAASO (Cao et al. 2025c), IceTop (Aartsen et al. 2019), CALET (Adriani et al. 2022), DAMPE (An et al. 2019), ISS-CREAM (Choi et al. 2022), NUCLEON-IC, and NUCLEON-KLEM (Grebenyuk et al. 2019). The contribution expected from a one-zone model with the Galactic diffusion is shown as dashed lines. The left and right panels show the results for standard case with $\eta_{CR} = 0.1$, and for the maximum-efficiency case, in which η_{CR} is adjusted to reproduce the observed gamma-ray flux at 100 TeV when possible. The fluxes of MAXI J1820+070 and Cygnus X-3 are multiplied by a factor 10^3 in the left panel, and by a factor 10^3 and 10^2 respectively in the right panel. This rescaling reduces the dynamic range of the y-axis so as to improve readability.

Constraints on hadronic emission from microquasars detected by LHAASO

Vecchiotti et al., A&A (2026)

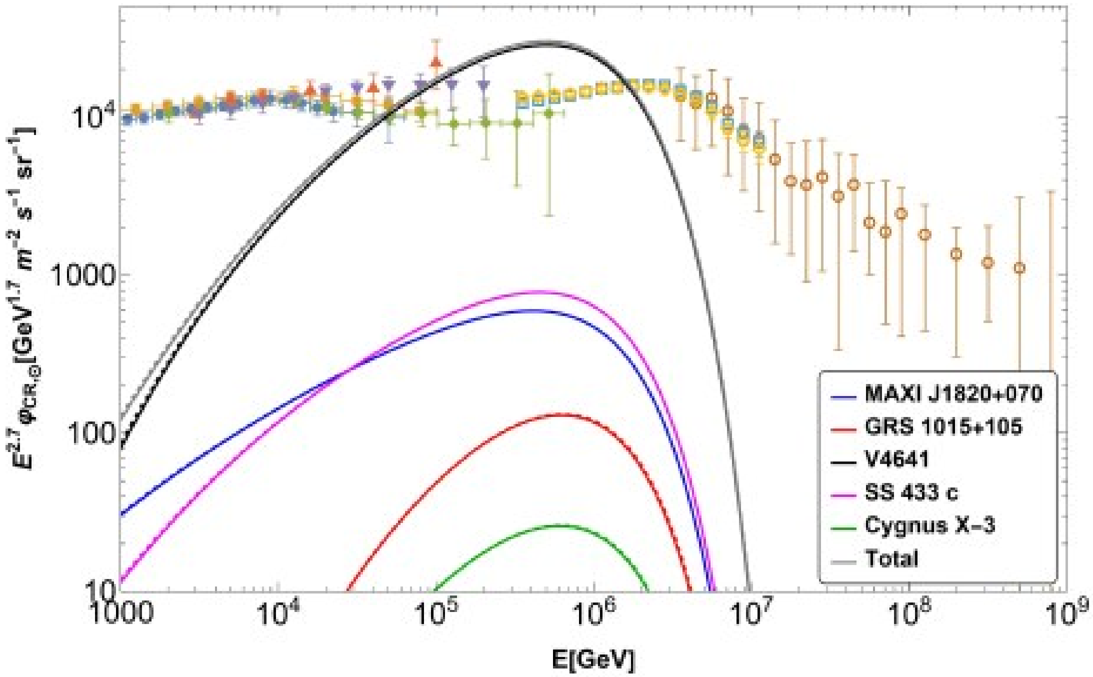

Fig. 4: Same as Figure 3 for our standard case $\eta_{CR} = 0.1$ and continuous injection over 1 Myr.

Constraints on hadronic emission from microquasars detected by LHAASO

Vecchiotti et al., A&A (2026)

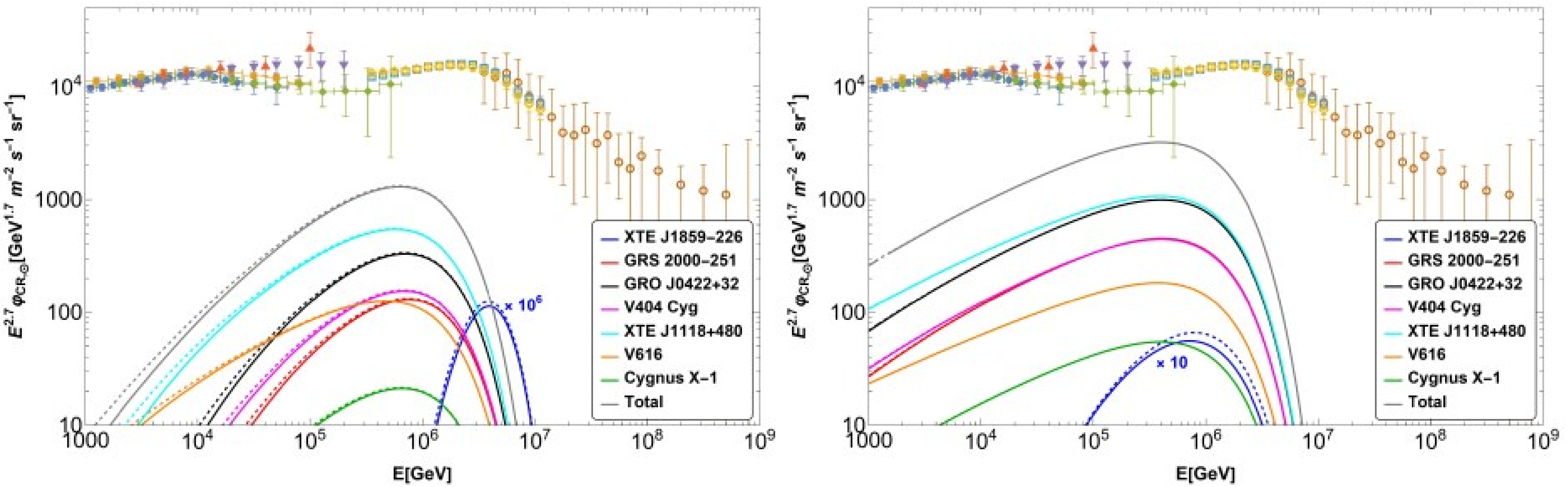

Fig. 6: Upper limit on the contribution to the CR spectrum for the microquasars undetected for LHAASO. The left (right) panel represent the contribution in case of continuous injection over 100 kyr (1 Myr). The flux of XTE J1859+226 is scaled by factors of 10^6 (left panel), and 10 (right panel), to reduce the dynamic range of the y-axis and improve visual clarity.

Sources associated to pulsars in LHAASO Catalogue

LHAASO Collaboration, ApJS 271, 25 (2024)

Table 4. 1LHAASO sources associated pulsars

Source name	PSR name	Sep.(°)	d (kpc)	τ_c (kyr)	$\dot{E}$ (erg s^{-1})	P_c	Identified type in TeVCat
1LHAASO J0007+7303u	PSR J0007+7303	0.05	1.40	14	4.5e+35	7.3e-05	PWN
1LHAASO J0216+4237u	PSR J0218+4232	0.33	3.15	476000	2.4e+35	3.6e-03	
1LHAASO J0249+6022	PSR J0248+6021	0.16	2.00	62	2.1e+35	1.5e-03	
1LHAASO J0359+5406	PSR J0359+5414	0.15	-	75	1.3e+36	7.2e-04	
1LHAASO J0534+2200u	PSR J0534+2200	0.01	2.00	1	4.5e+38	3.2e-06	PWN
1LHAASO J0542+2311u	PSR J0543+2329	0.30	1.56	253	4.1e+34	8.3e-03	
1LHAASO J0622+3754	PSR J0622+3749	0.09	-	208	2.7e+34	2.5e-04	PWN/TeV Halo
1LHAASO J0631+1040	PSR J0631+1037	0.11	2.10	44	1.7e+35	3.5e-04	PWN
1LHAASO J0634+1741u	PSR J0633+1746	0.12	0.19	342	3.3e+34	1.3e-03	PWN/TeV Halo
1LHAASO J0635+0619	PSR J0633+0632	0.39	1.35	59	1.2e+35	9.4e-03	
1LHAASO J1740+0948u	PSR J1740+1000	0.21	1.23	114	2.3e+35	1.4e-03	
1LHAASO J1809-1918u	PSR J1809-1917	0.05	3.27	51	1.8e+36	6.2e-04	
1LHAASO J1813-1245	PSR J1813-1245	0.01	2.63	43	6.2e+36	6.3e-06	
1LHAASO J1825-1256u	PSR J1826-1256	0.09	1.55	14	3.6e+36	1.6e-03	
1LHAASO J1825-1337u	PSR J1826-1334	0.11	3.61	21	2.8e+36	2.8e-03	PWN/TeV Halo
1LHAASO J1837-0654u	PSR J1838-0655	0.12	6.60	23	5.6e+36	2.2e-03	PWN
1LHAASO J1839-0548u	PSR J1838-0537	0.20	-	5	6.0e+36	6.1e-03	
1LHAASO J1848-0001u	PSR J1849-0001	0.06	-	43	9.8e+36	1.2e-04	PWN
1LHAASO J1857+0245	PSR J1856+0245	0.16	6.32	21	4.6e+36	3.1e-03	PWN
1LHAASO J1906+0712	PSR J1906+0722	0.19	-	49	1.0e+36	5.9e-03	
1LHAASO J1908+0615u	PSR J1907+0602	0.23	2.37	20	2.8e+36	6.8e-03	
1LHAASO J1912+1014u	PSR J1913+1011	0.13	4.61	169	2.9e+36	1.5e-03	
1LHAASO J1914+1150u	PSR J1915+1150	0.09	14.01	116	5.4e+35	1.8e-03	
1LHAASO J1928+1746u	PSR J1928+1746	0.04	4.34	83	1.6e+36	1.6e-04	
1LHAASO J1929+1846u	PSR J1930+1852	0.29	7.00	3	1.2e+37	2.6e-03	PWN
1LHAASO J1954+2836u	PSR J1954+2836	0.01	1.96	69	1.1e+36	1.6e-05	PWN
1LHAASO J1954+3253	PSR J1952+3252	0.33	3.00	107	3.7e+36	6.7e-03	
1LHAASO J1959+2846u	PSR J1958+2845	0.10	1.95	22	3.4e+35	2.8e-03	PWN
1LHAASO J2005+3415	PSR J2004+3429	0.25	10.78	18	5.8e+35	9.9e-03	
1LHAASO J2005+3050	PSR J2006+3102	0.20	6.04	104	2.2e+35	9.2e-03	
1LHAASO J2020+3649u	PSR J2021+3651	0.05	1.80	17	3.4e+36	1.5e-04	PWN
1LHAASO J2028+3352	PSR J2028+3332	0.36	-	576	3.5e+34	8.0e-03	
1LHAASO J2031+4127u	PSR J2032+4127	0.08	1.33	201	1.5e+35	1.0e-03	PWN
1LHAASO J2228+6100u	PSR J2229+6114	0.27	3.00	10	2.2e+37	2.2e-03	PWN
1LHAASO J2238+5900	PSR J2238+5903	0.07	2.83	27	8.9e+35	3.0e-04	

LHAASO Collaboration, Science (2021)

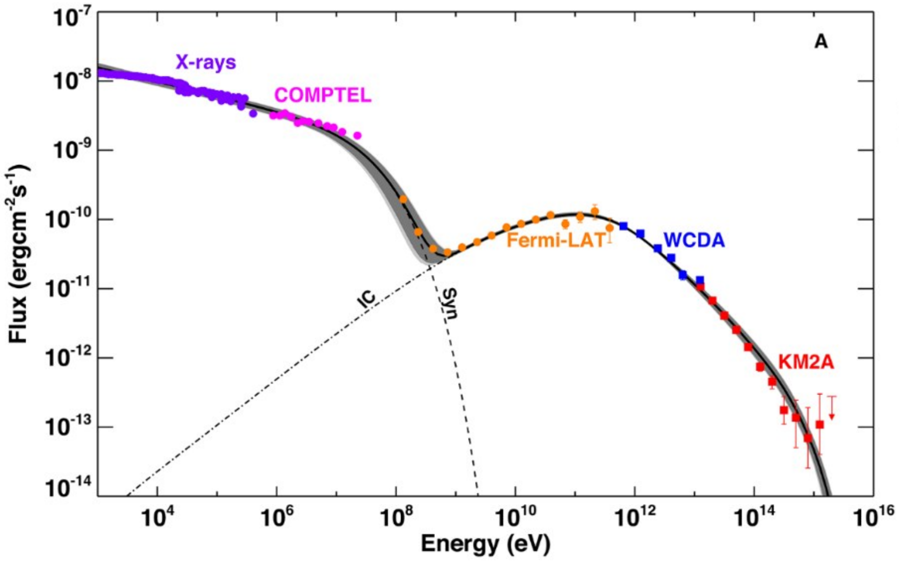

Crab : Leptonic PeVatron

Crab Nebula - Sketch

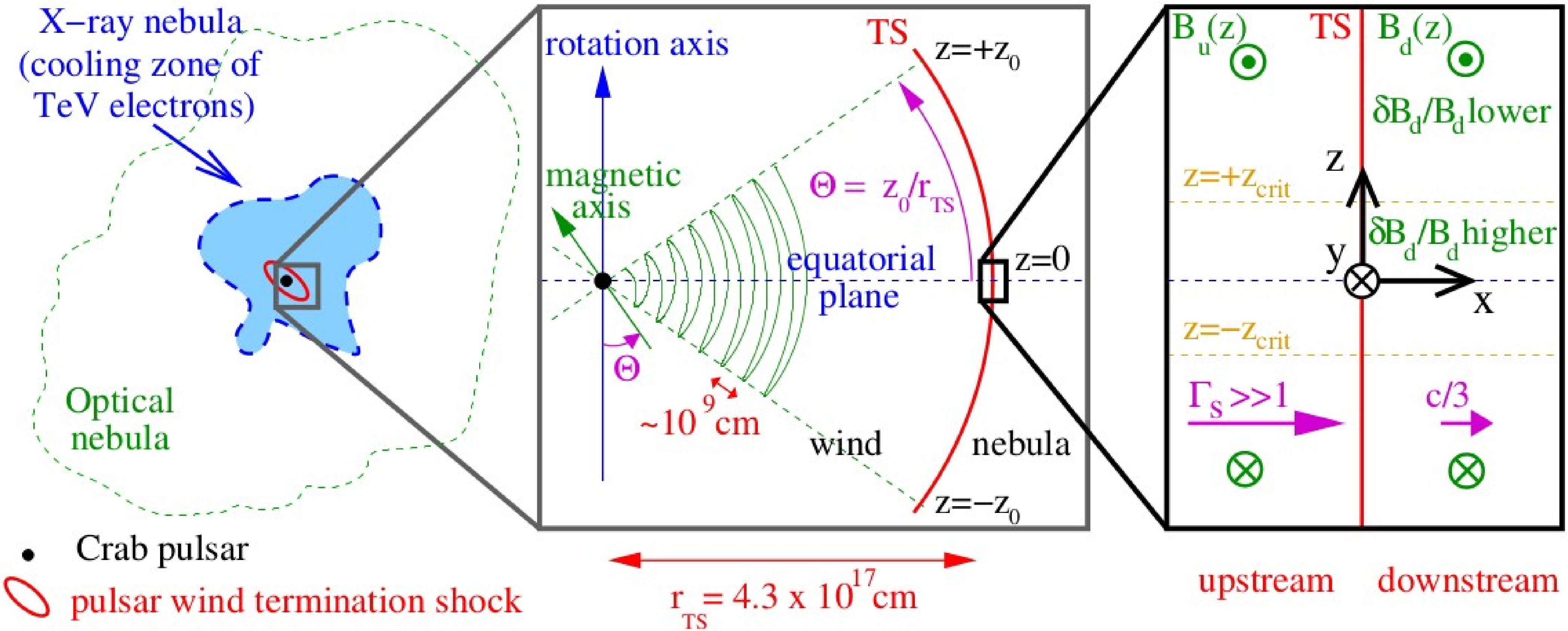

Giacinti & Kirk, ApJ **863**, 18 (2018)

Magnetic reconnection

Sironi & Spitkovsky (2014):

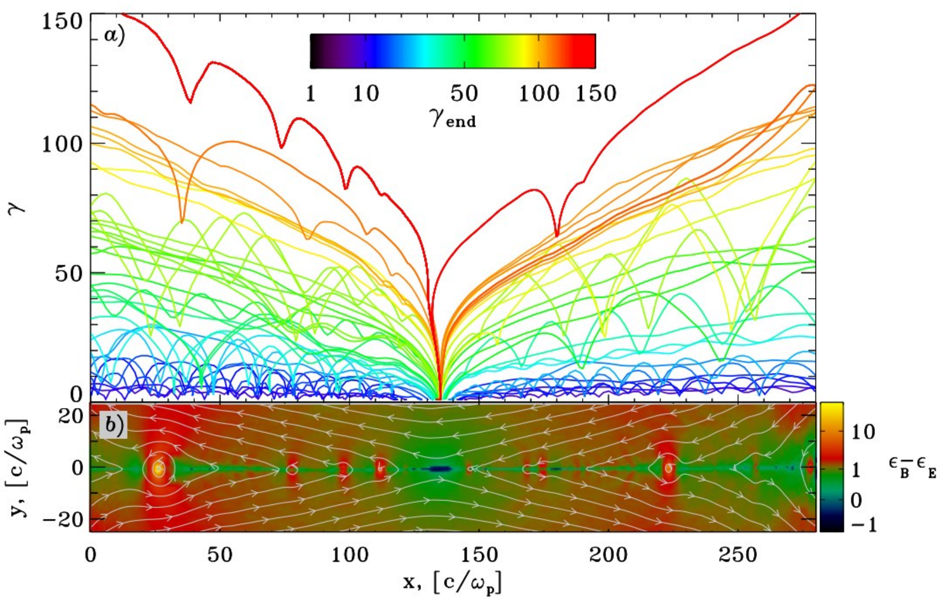

Lu et al. (2021):

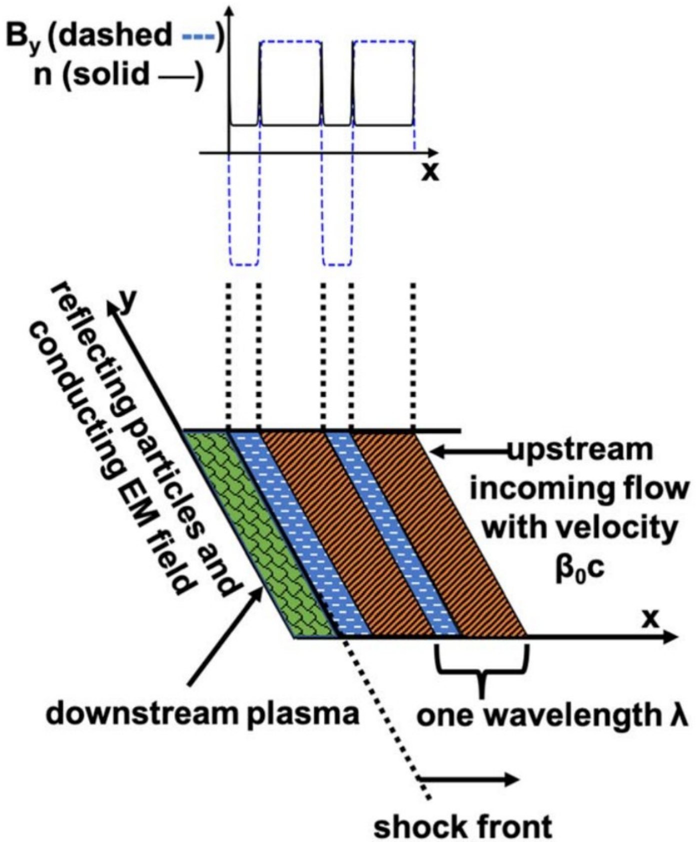

Numerical simulations

<u>**POSITRONS:**</u>

<u>**ELECTRONS:**</u>

(roles exchanged with opposite pulsar polarity)

No/little acceleration

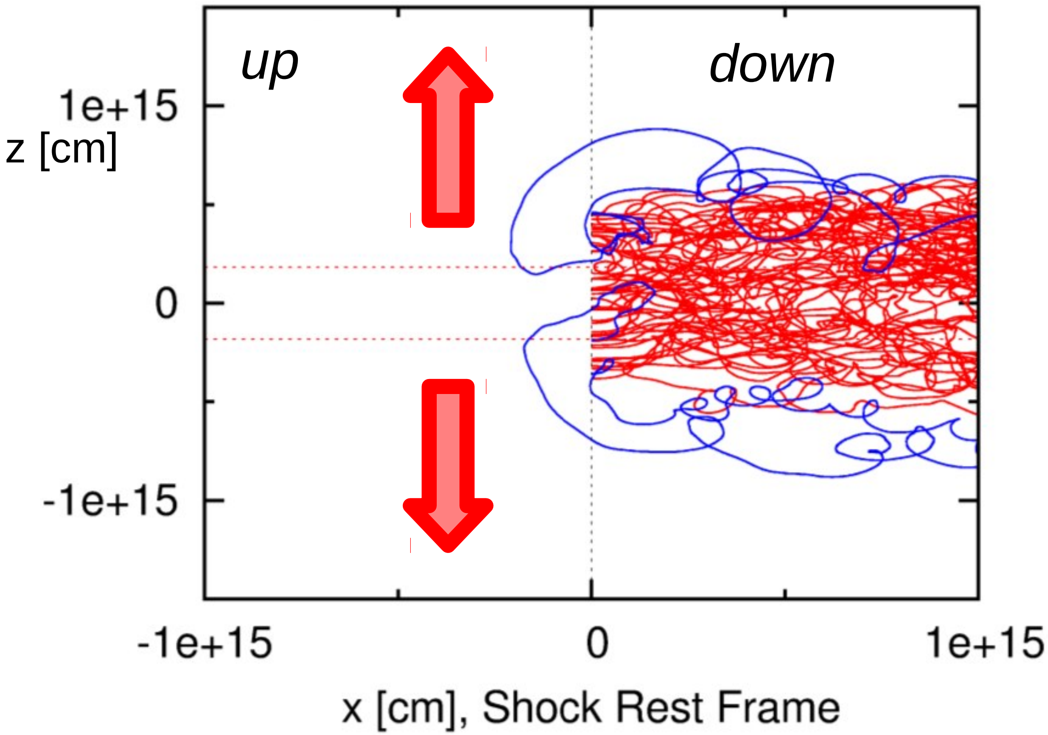

Efficient acceleration to VHE !

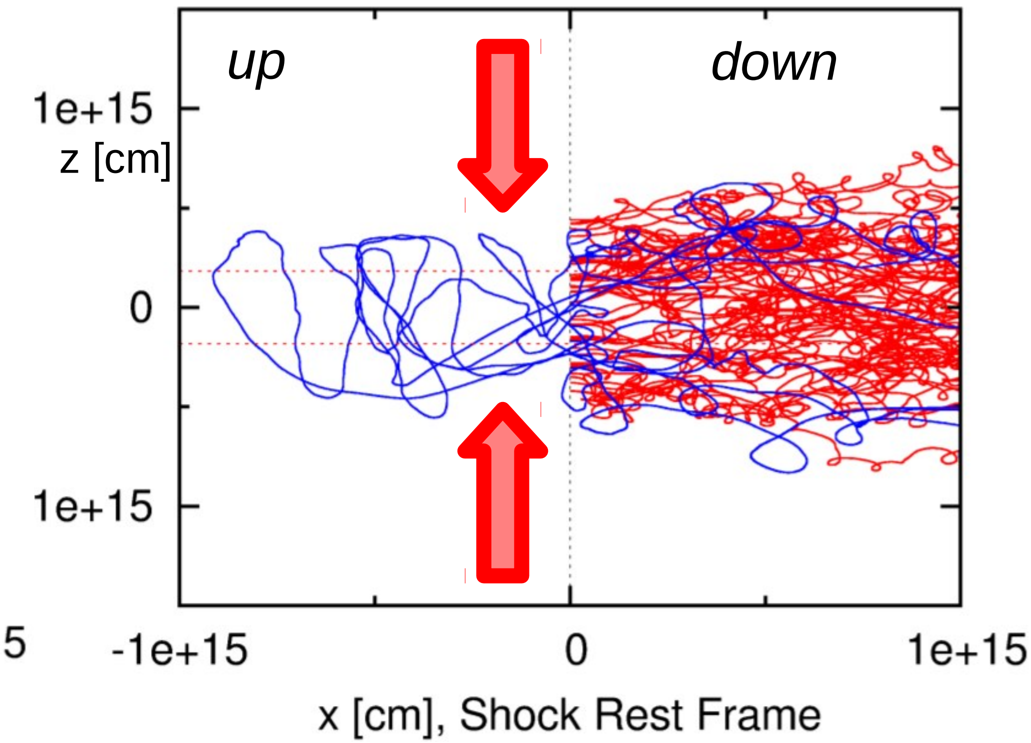

GG & Kirk, ApJ **863**, 18 (2018)

Cerutti & Giacinti, A&A **642**, A123 (2020); A&A **656**, A91 (2021)

HAWC observ. of Geminga & Monogem

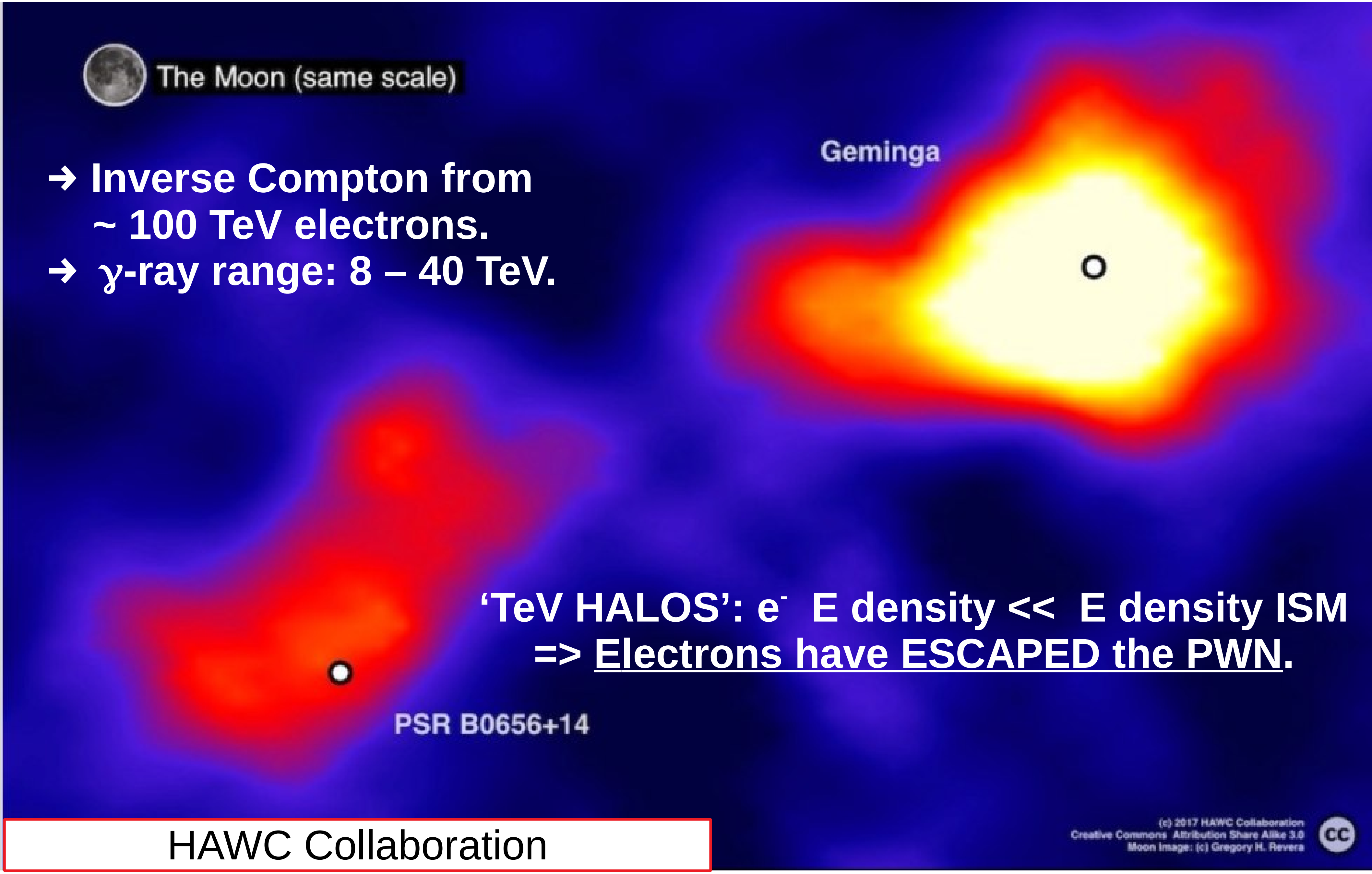

- ➔ Inverse Compton from ~ 100 TeV electrons.
- ➔ γ-ray range: 8 – 40 TeV.

'TeV HALOS': e^- E density << E density ISM
=> <u>Electrons have ESCAPED the PWN</u>.

HAWC Collaboration

LHAASO’s peanut-shaped source

LHAASO Coll.,
arXiv:2510.06786

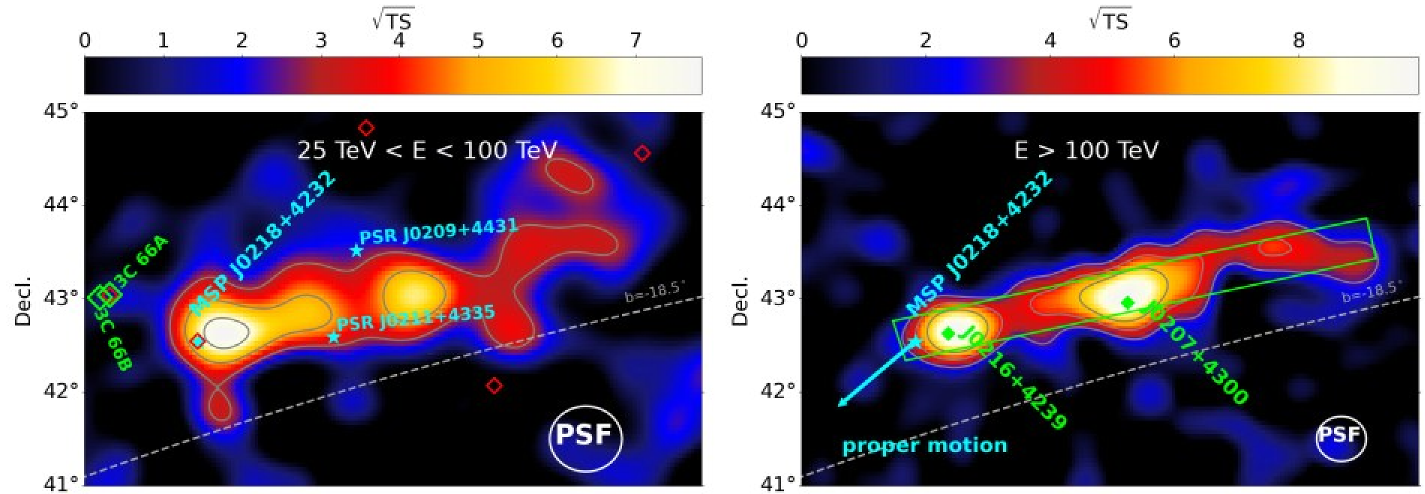

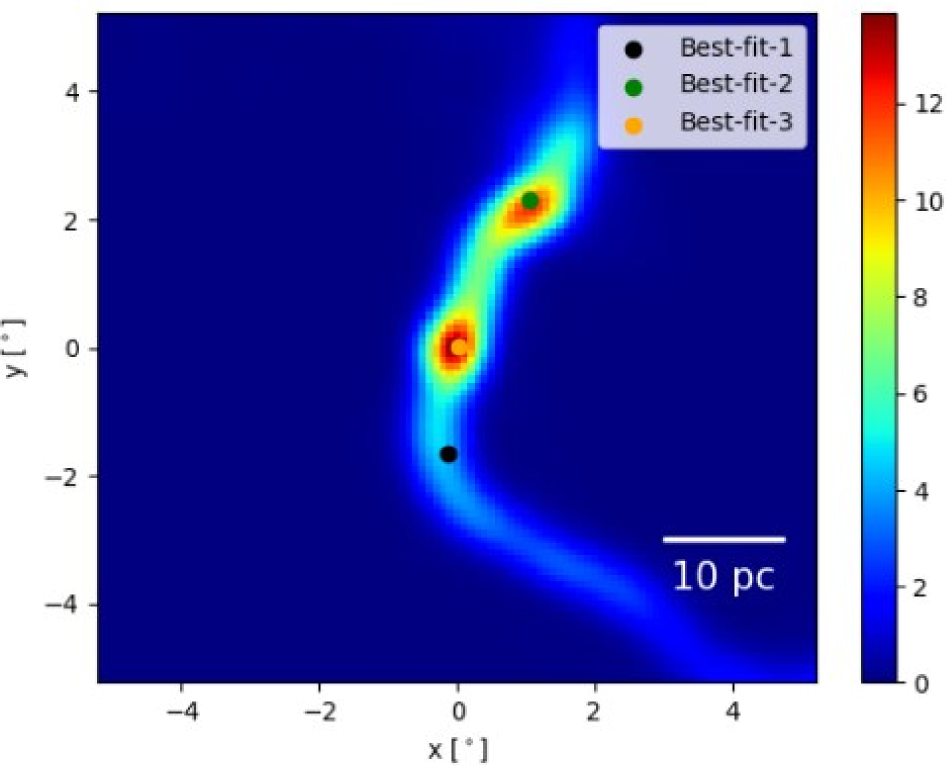

Bao, GG, Liu, Zhang & Chen, PRL (2025)

Bao, Liu, GG, Zhang & Chen, PRD (2025)

→ Secondary sources can appear. They are "mirages", where the magnetic field bends along the observer LOS

Diffuse Galactic VHE γ-ray emission:

Can it constrain the nature of hadronic PeVatrons ?

The sky at ~ 10 TeV – 1 PeV: Diffuse emission from LHAASO

LHAASO Collaboration, Phys. Rev. Lett. 131, 151001 (2023)

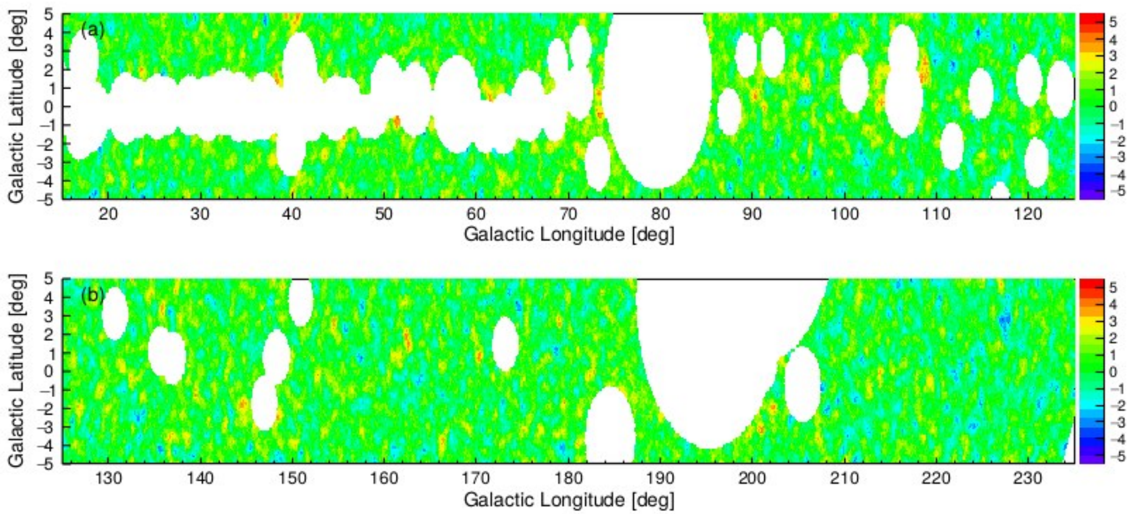

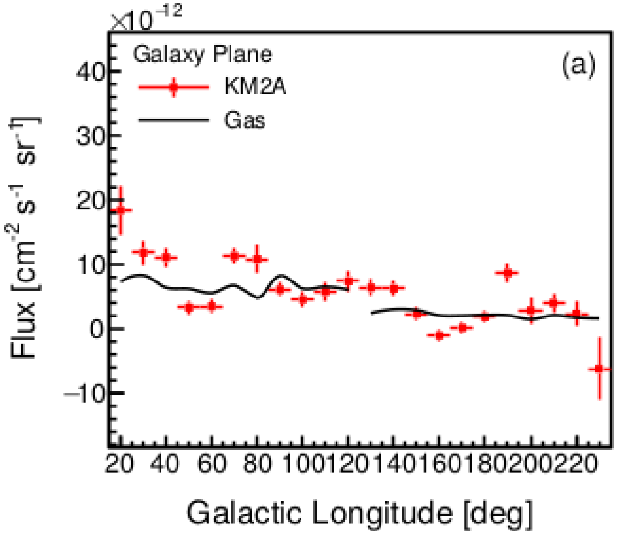

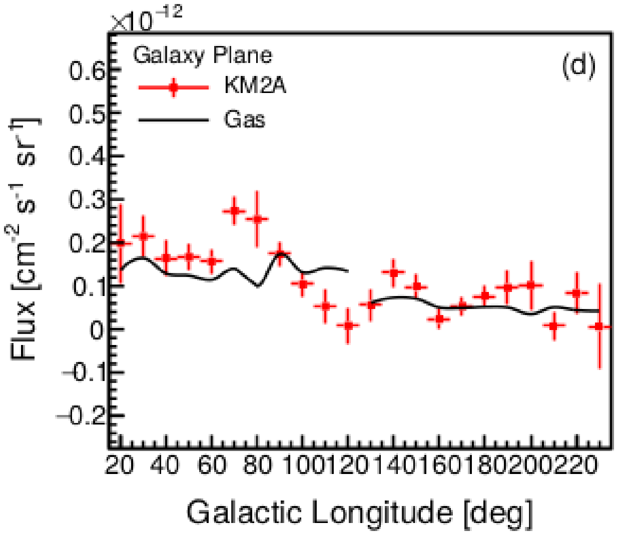

Emission in Galactic longitude does not follow target gas…

→ Leptonic origin?
→ Stochasticity of CR injection?

Comparing γ and ν observations

IceCube Collaboration, Science (2023)

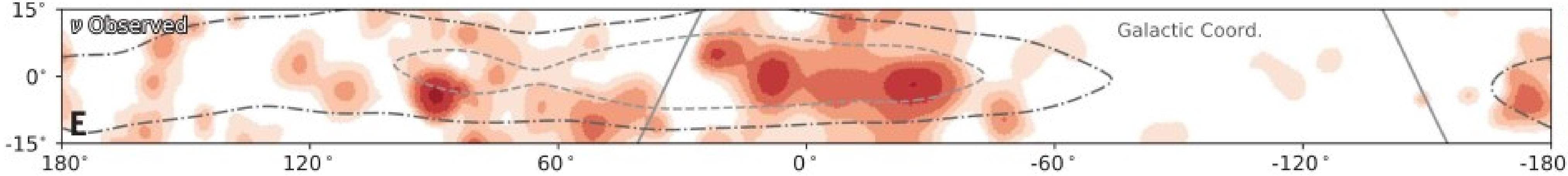

Fang & Murase, ApJL (2023)

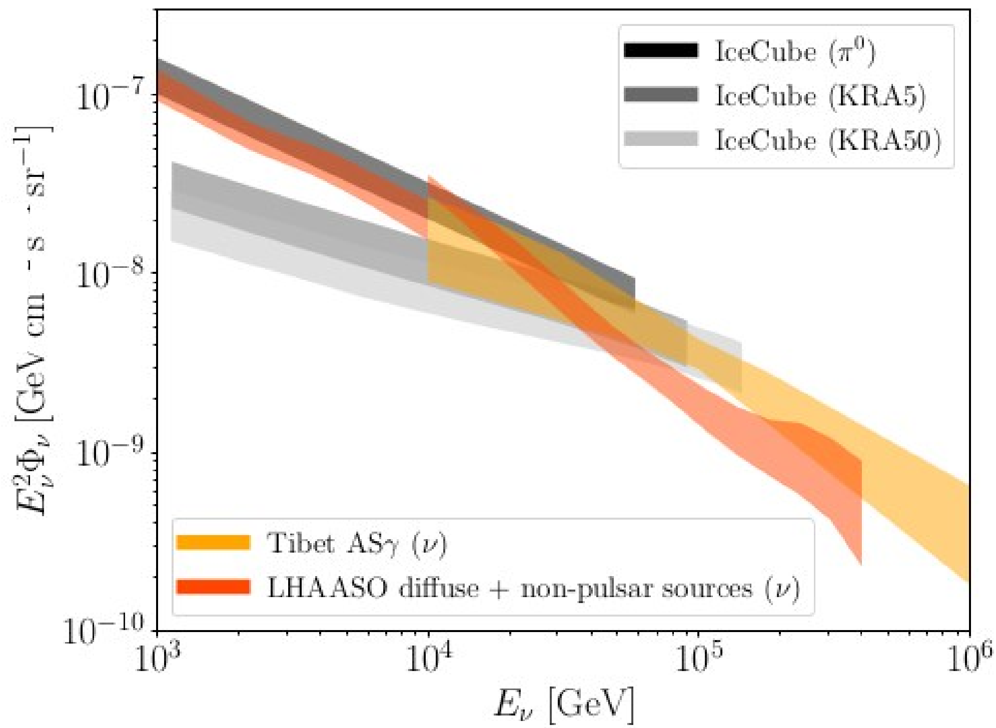

=> LHAASO diffuse emission should come mainly from hadronic interactions above ~ 30 TeV.

Impact of unresolved sources (PWNe)

Kaci, Giacinti, Semikoz, ApJ Lett. 975, L6 (2024)

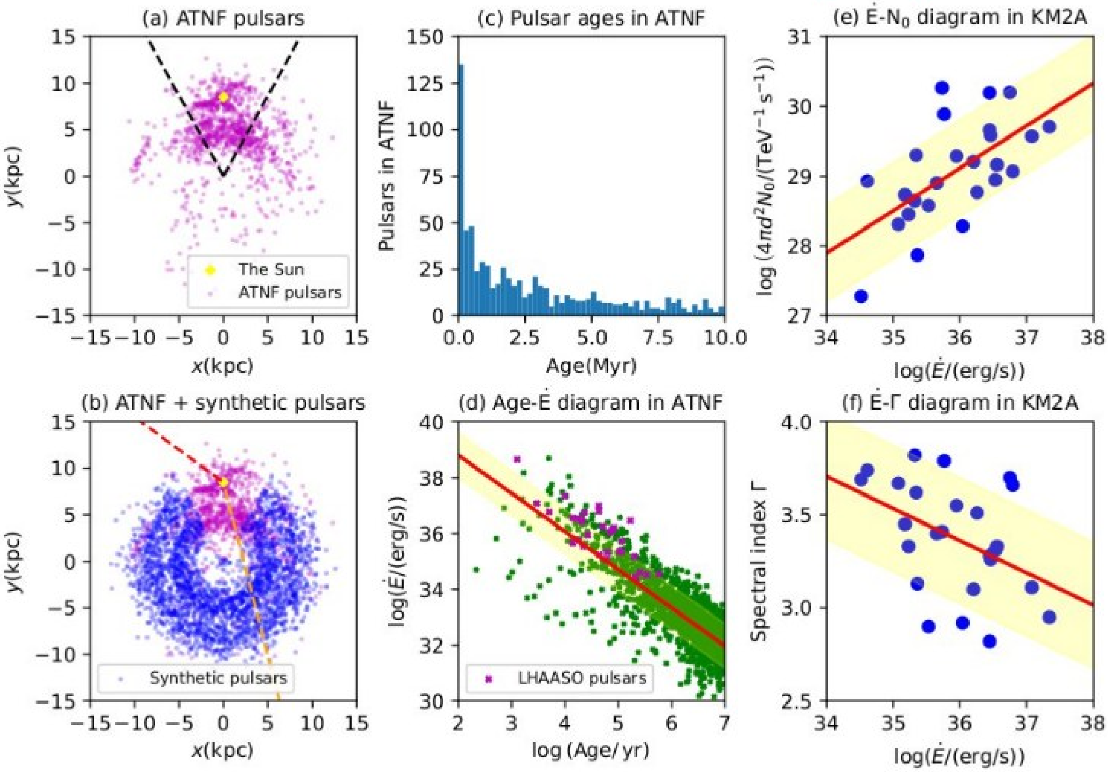

- Use ATNF catalog and complete it.
- Generate a VHE gamma-ray emission similar to that measured by KM2A for each source.
- Constrain the gamma-ray emission to be below KM2A sensitivity.
- Use the same masks as LHAASO.
- Compare the contribution of unresolved sources to the total flux measured by KM2A.

Upper Limits unresolved PWNe/halos

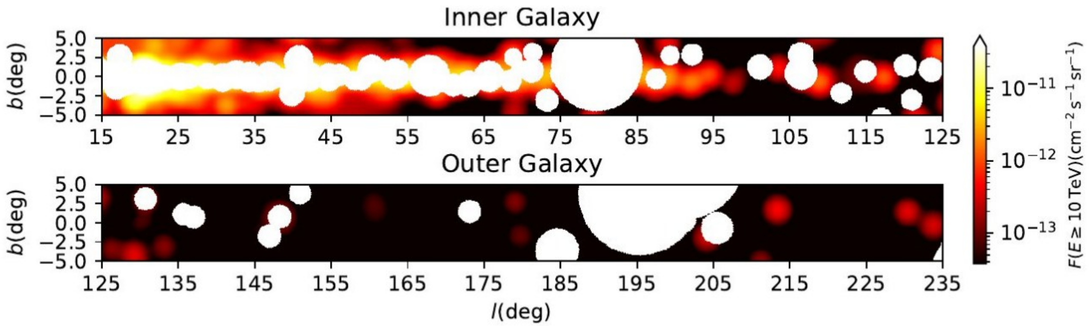

Kaci, Giacinti, Semikoz, ApJ Lett. 975, L6 (2024) ; + Submitted (2026)

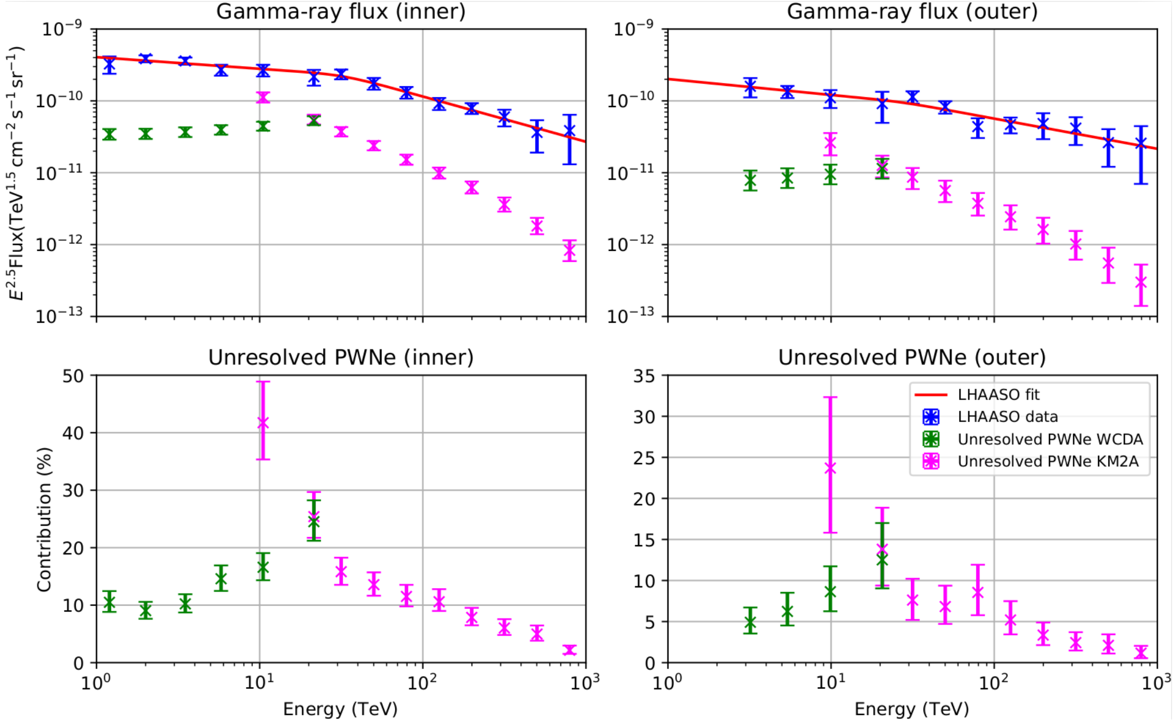

→ The contribution of PWNe to the diffuse background is rather negligible.

→ It peaks at 30% at most at 25TeV in the inner Galaxy.

Diffuse VHE γ-ray emission from discrete sources

SIMULATION:

Kaci & Giacinti, JCAP 01, 049 (2025)

Isotropic and homogeneous diffusion

1) GALPROP-like (d=1/3) :

$$D(E) = 10^{28} D_{28} \left(\frac{R}{3GV}\right)^{\delta} cm^2/s$$

$$D_{28} = 1.33 \times \frac{H}{kpc}$$

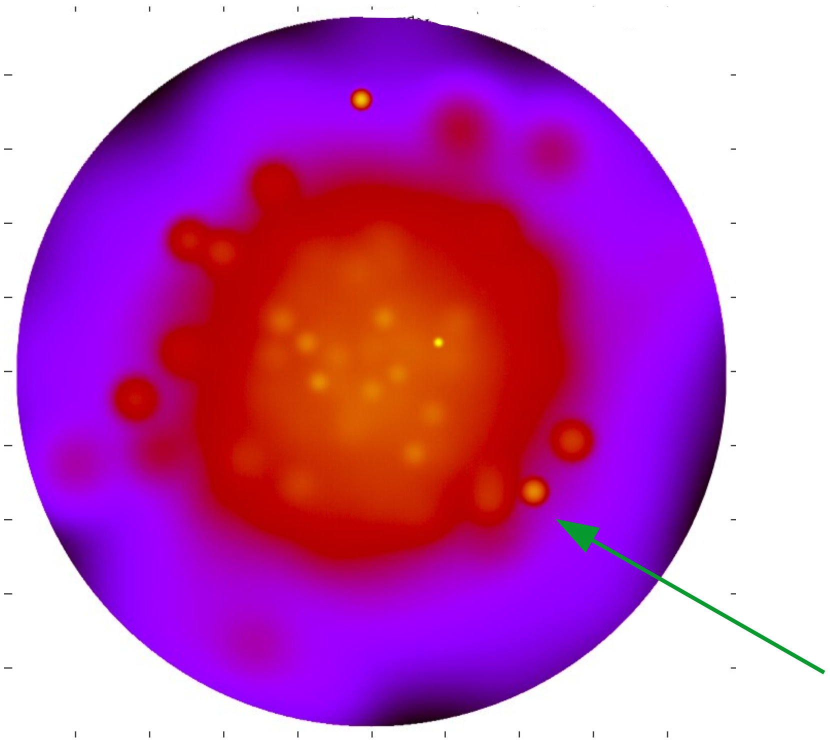

Cosmic-ray flux at Earth and B/C ratio satisfied

Discrete injection of cosmic rays

Sky Maps and sources

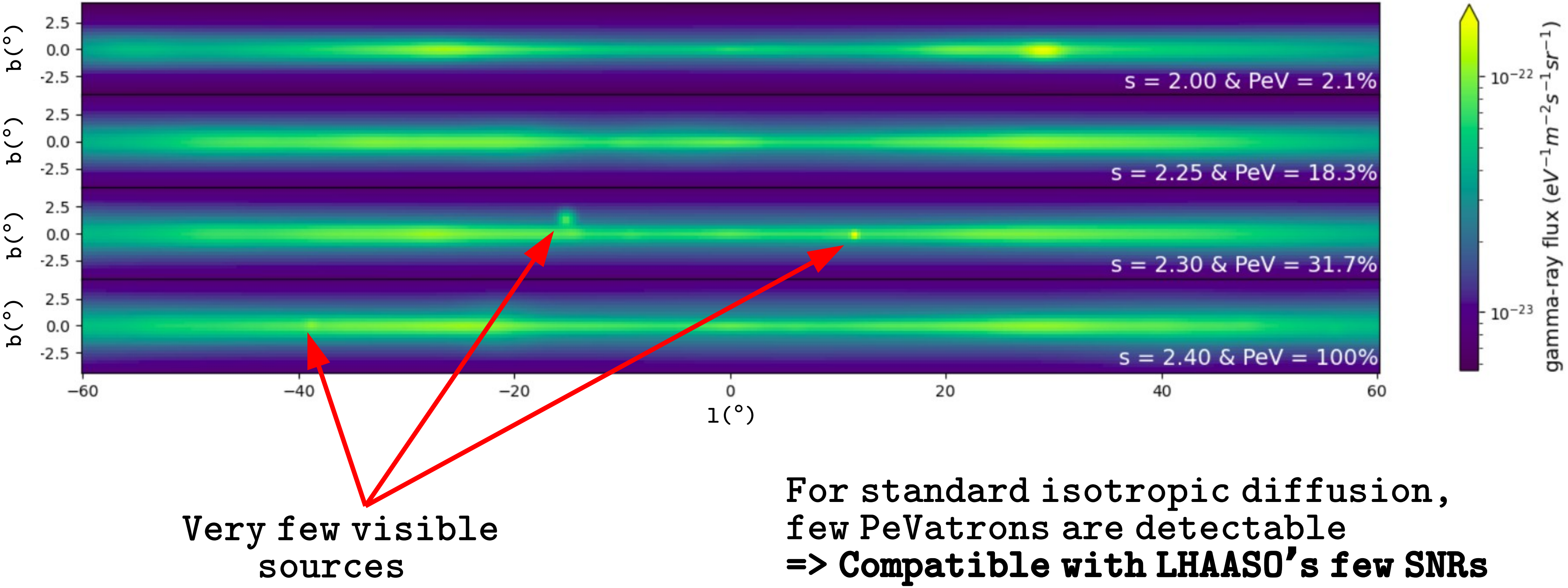

For standard isotropic diffusion, few PeVatrons are detectable
=> Compatible with LHAASO's few SNRs

Kaci & Giacinti, JCAP 01, 049 (2025)

Microquasars as Galactic super-PeVatrons

Kaci, Giacinti, Aharonian & Wang, Submitted to PRL

- Assume a population of ~ 10 microquasars acreting close to their Eddington limit at any given time (Need for a huge power, but the number of candidates is limited).
- Assume a lifetime of ~ 100 kyr for microquasars acting as super-PeVatrons.
- Simulate their contribution in the entire Galaxy following S. Kaci & G. Giacinti (2025).
- Compare to observations.

Cosmic-ray spectrum

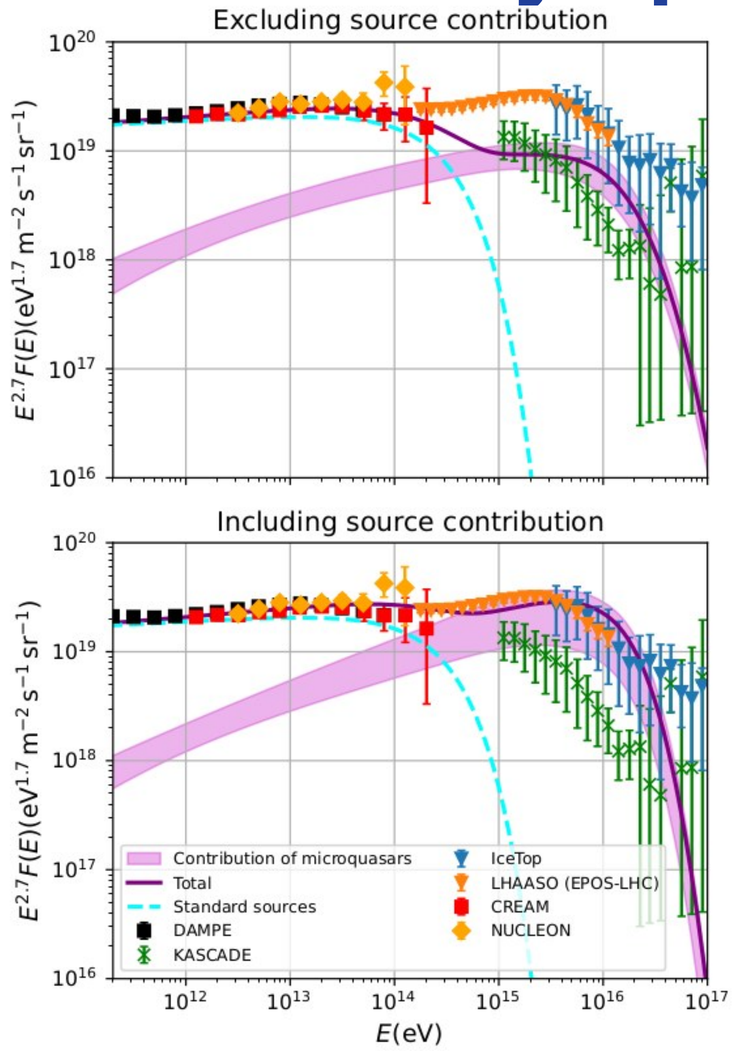

Kaci, Giacinti, Aharonian & Wang, Submitted to PRL

- The flux of the sea of cosmic rays originating from microquasars cannot be neglected.
- Microquasars can entirely account for the cosmic-ray flux around the knee and above.
- The 10TeV bump and the hardening at 300TeV arise naturally.

Detectable sources

Kaci, Giacinti, Aharonian & Wang, Submitted to PRL

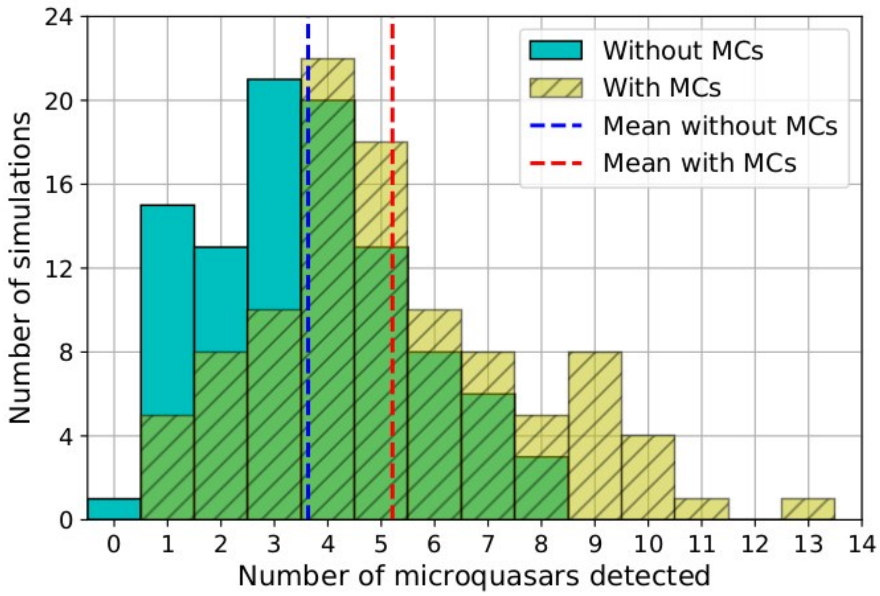

- The number of detectable microquasars in the Galaxy with and without molecular clouds above 100TeV is compatible with the LHAASO observation of 6 sources.
- Some of the observed sources might be leptonic. This will be investigated with neutrino observations.

Diffuse gamma-ray emission

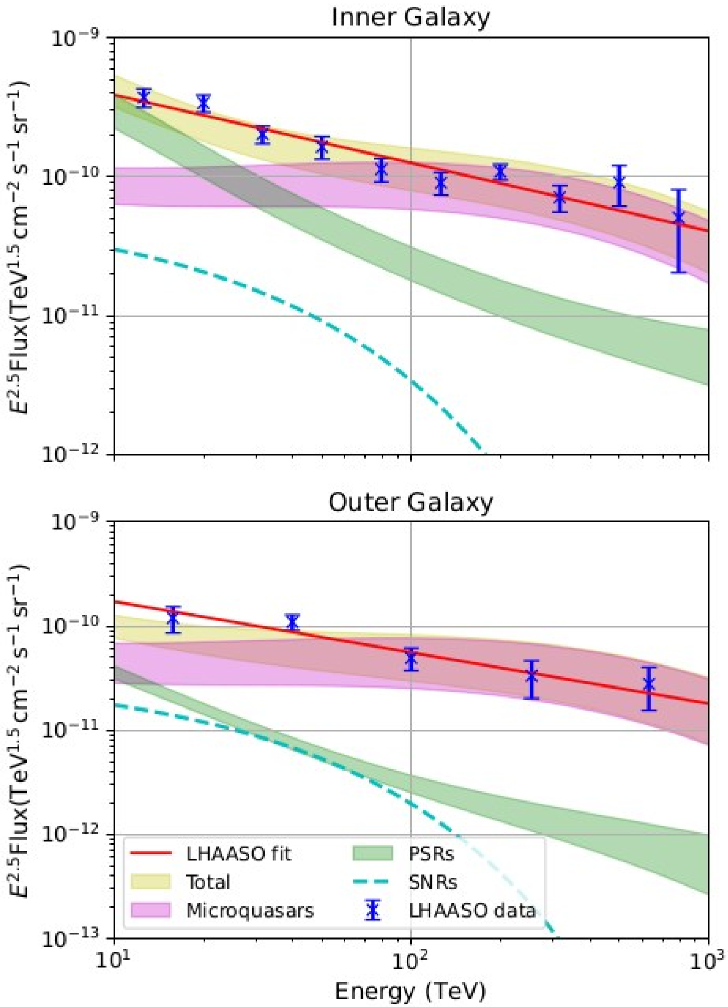

Kaci, Giacinti, Aharonian & Wang, Submitted to PRL

- In the outer Galaxy the contribution of microquasars almost entirely account for the diffuse gamma-ray flux.
- In the inner Galaxy, microquasars can explain gamma-ray data with a minimal contribution from unresolved pulsars above 50TeV.

Conclusions

→ **We are getting closer to understanding the nature of Galactic PeVatrons.**

→ **Most LHAASO sources seem to be leptonic (PWNe),**
… while the diffuse background is mostly hadronic

→ Standard PWNe are probably not the long-sought PeVatrons...

→ … But interesting new candidates have emerged: **CC SNe, Superbubbles, Microquasars**

→ **Clumpy diffuse γ-ray background at VHE**

→ **Unresolved PWNe/halos**: Minor contribution

→ ~ 10 powerful **microquasars can fit CR spectrum at > 200 TeV and diffuse γ-ray bkg.**